Estuarine, Coastal and Shelf Science
April 2014, Volume 219, Pages 176-188
https://doi.org/10.1016/j.ecss.2019.02.014
https://archimer.ifremer.fr/doc/00481/59238/

Physiological and behavioral responses of phytoplankton communities to nutrient availability in a disturbed Mediterranean coastal lagoon

Leruste A. [1, 2, *], Pasqualini V. [1], Garrido M. [1, 3], Malet Nathalie [4], De Wit R. [2], Bec Beatrice [2]

[1] UMR SPE CNRS/UMS Stella Mare CNRS, Université de Corse, 20250, Corte, France
[2] MARine Biodiversity Exploitation and Conservation MARBEC, Université de Montpellier, IRD, Ifremer, CNRS. Bât. 24, Place Eugène Bataillon, 34095, Montpellier cedex 5, France
[3] Environmental Agency of Corsica, 7 Avenue Jean Nicoli, 20250, Corte, France
[4] Ifremer, Laboratoire Environment Resources Provence-Azur-Corse (LER/PAC), Station de Bastia, Z.I. Furiani, Immeuble Agostini, 20600, Bastia, France

* Corresponding author : A. Leruste, email address : leruste-calpena_a@univ-corse.fr

Abstract :

Short-term bioassays were conducted in Biguglia lagoon (Corsica) to study the physiological and behavioral responses of phytoplankton to N- and P-availability. Natural communities were collected in two stations representative of the two sub-basins, at three periods with contrasting environmental characteristics to address the impact of seasonal variability. These samples were separately enriched with a full N and P enrichment, and with enrichments minus N or minus P. Phytoplankton size structuration, diversity, and growth of the total phytoplankton, the micro-, nano- and ultraphytoplankton were evaluated using spectrofluorimetry, and optical microscopy. Results showed that the communities were fueled by $NO3^-$ in the wet periods (autumn and spring) and $NH4^+$ in summer. The phytoplankton communities displayed highest cell size in autumn, with high abundances of nanoflagellates, and smallest cell size in summer with a large dominance of phycocyanin-rich picocyanobacteria. Blooms of dinoflagellates also occurred during the wet periods, coinciding with high N:P ratios. The full enrichment has not stimulated phytoplankton growth in autumn, suggesting the importance of other controlling factors such as light, a possible $NH4^+$ inhibition or the use of mixotrophic abilities. In spring, communities have displayed single P-limitation in the northern basin and different N and P co-limitations in the southern basin. In summer, the full enrichment consistently stimulated the growth of all cell sizes. The communities showed high N and P co-limitations, which is consistent with growing observations in aquatic ecosystems, and reflects the different functional responses of phytoplankton communities to the nutrient availability.

Graphical abstract

Chlosrophyll *a* (Chl *a*) concentration, DIN:DIP ratio, main taxa/morphotypes, response to the full nutrient enrichment, and N- and/or P-limitation during the three bioassay periods in the two stations representatives of the Northern and the Southern basins of Biguglia lagoon.

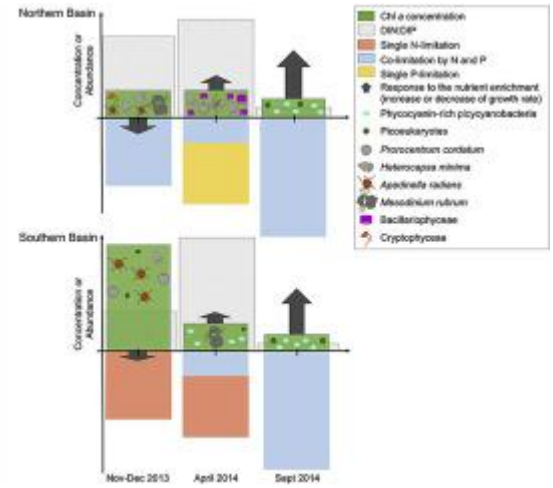

Highlights

► Freshwater inputs from the watershed strongly influenced the phytoplankton of Biguglia lagoon.
► Nanoflagellates dominated phytoplankton communities in autumn and spring with high N:P ratios.
► Phycocyanin-rich picocyanobacteria bloomed in the sampling in September with low N:P ratios.
► Phytoplankton showed differential responses to nutrient enrichments and induced limitations.
► Phytoplankton was generally co-limited by N and P, with exceptions depending on seasons.

Keywords : growth rate, dilution experiment, eutrophication, functional traits

1. Introduction

Coastal lagoons are very productive ecosystems at the sea-land interface hosting a high degree of biodiversity and providing numerous ecosystem services for human wellbeing (Barbier et al., 2011). These services confer a high economical value for the coastal lagoons, *e.g*. as water and food supply (fishing, shellfish farming), tourism and recreation (Franco et al., 2010; Rochette et al., 2010). However, because of their location in densely populated littoral areas and the services they provide, coastal lagoons and their surroundings have been increasingly exploited for human uses. Overexploitation combined with the hydromorphology of these semi-enclosed systems and climate change have increased their vulnerability to anthropogenic impacts. Hence, coastal lagoons are among the most threatened ecosystems (Nixon, 2009). This threat is mainly associated with changes in their hydrology and with an increase of nutrients and pollutants inputs from sewage effluents and watershed run-off (Mouillot et al., 2000; Cloern, 2001). Due to shallowness and confinement, these inputs result in high concentration of nutrients and pollutants in coastal lagoons, thereby exacerbating their degradation (Donald et al., 2013).

An excessive or unbalanced input of nutrients disturbs the community of primary producers, leading to an increase of the eutrophication processes and to drastic changes in the biodiversity of the autotrophic compartment. Thus, it may promote fast-growing opportunistic algae in the first place and finally phytoplankton at the expense of benthic organisms such as macrophytes, and may result in an increase of the frequency of harmful algal blooms (Schramm, 1999; Livingston, 2000; Le Fur et al., 2018). These changes in the composition of the autotrophic communities impact all the trophic levels, altering the ecosystem functioning (Cloern, 2001). High nutrient inputs can also, through an accumulation of macroalgal or phytoplankton biomass, lead to the development of dystrophic crisis and hypoxia and anoxia

events, having dramatic impacts on all the living organisms (Cloern, 2001). Therefore, the management of a eutrophicated coastal lagoon needs to target the reduction of nutrient loadings. In addition, knowledge is required about the availability of nutrients within lagoons and the autotrophic communities responses (Duarte et al., 2000; Glibert et al., 2015). This allows to assess the resilience of the aquatic communities, and to estimate the critical nutrient loading for the ecosystem (Pasqualini et al., 2017; Le Fur et al., 2018).

Phytoplankton represents the basis of food webs and biochemical cycles, and is generally the first autotrophic compartment responding to a change of nutrient availability (Leruste et al., 2016). Understanding how the ecosystem functioning influences the composition of phytoplankton communities and their growth mechanisms is indispensable (Livingston, 2000; Paerl et al., 2003). Hence, it is particularly important to understand and predict how N and P inputs affect the growth and community assembly of phytoplankton. These responses are indicators of water quality, and are consequently informative for water management (Duarte et al., 2000; Reed et al., 2016). Morphological and physiological traits such as cell size and maximal growth rates shape the phytoplankton functional responses to nutrient availability. Small-size fast-growing algae are competitive at low nutrient concentrations and low light, while larger cells can generally thrive under a pulsed nutrient supply and higher light intensities (Litchman et al., 2007; Bec et al., 2011; Andersen et al., 2015). The community composition also reflects which nutrients are available. Diatoms are particularly competitive for nitrate, while green algae and picocyanobacteria are more competitive for ammonium. The latter often originates from regenerated internal sources. Dinoflagellates can develop even under dissolved inorganic nutrient limitation, because of their relatively low growth rates and potential mixotrophic abilities (Litchman et al., 2007; Glibert et al., 2015).

The general aim of this study was to explore the responses of the phytoplankton communities of a disturbed Mediterranean coastal lagoon to the nutrient availability. Therefore, we choose Biguglia lagoon, which is the largest lagoon on the island of Corsica, as the study site. This Mediterranean lagoon has been increasingly impacted since 1980 by a strong increase of the human population density, industrial and agricultural uses in its catchment and its surrounding areas. This lagoon receives particularly high amounts of nitrate from runoffs, tributaries, and from groundwater flows from a coastal aquifer connected with the lagoon (Erostate et al., 2018). Biguglia lagoon also displays a high confinement and restricted exchanges with the Tyrrhenian Sea that have induced higher levels of nutrient concentration than in most other French Mediterranean lagoons these last decades (Souchu et al., 2010; Pasqualini et al., 2017). Hence, the lagoon has experienced strong changes in its ecological state, *i.e.* increasing eutrophication and pollutant levels linked with changes in the composition of its autotrophic community (Mouillot et al., 2000; Pasqualini et al., 2017). Moreover, a dystrophic crisis associated with a bloom of toxic cyanobacteria in 2007 has raised the awareness of the water quality in the lagoon among the responsible management authorities. Therefore, they have taken remediation measures to reduce the confinement in order to decrease the concentration of nutrients. This included the modification of the lagoon hydrology since 2009 to increase dilution processes (Cecchi et al., 2016; Garrido et al., 2016). However, so far, no efficient direct management measures have been implemented to reduce the external nutrient loadings that remain important and uncontrolled. Moreover, although the measures taken in 2009 may have helped the development of aquatic angiosperms (Pasqualini et al., 2017), these may have also promoted the occurrence of blooms of potentially toxic and or harmfull dinoflagellate species (Cecchi et al., 2016).

The specific objectives of this study were to describe in different seasons with contrasting environmental conditions including nutrient form and origin, (1) the structure of phytoplankton communities in Biguglia lagoon submitted to a strong anthropogenic impact in term of size classes and species diversity, and (2) their growth rate in response to various forms of nutrients inputs. These two observations illustrate phytoplankton functional responses to contrasting nutrient availability, and the latter specially reflects the vulnerability of the whole ecosystem to a short-term nutrient pulse. We experimentally incubated phytoplankton communities under *in situ* light and temperature conditions with enrichments containing N (NO_3^-, NH_4^+) and P (PO_4^{3-}), either in combination or separately to selectively induce either N- or P-limitation. Exploring the responses of phytoplankton communities to a change in nutrient availability helped understanding the impact of these changes on the ecosystem functioning.

2. Material and Methods

2.1. *Characterization of the study site*

Biguglia lagoon (42°36'N; 9°28'E) is a shallow brackish coastal lagoon (average depth 1.2 m), located on the East coast of Corsica, and separated from the Tyrrhenian Sea by a sandy beach barrier (Fig. 1). This choked lagoon *sensu* Kjerfve (1994) covers 14.5 km^2 with a single inlet in the north to the sea that consists of a 1.5 km long, narrow and shallow natural channel. Biguglia lagoon is divided into two sub-basins by a peninsula in its middle. Each of these sub-basins displays a specific hydrological functioning resulting in differences in salinity, nutrient concentrations and phytoplankton biomasses (Garrido et al., 2016).

The microtidal conditions, and the morphology of this inlet and its natural inclination to silt up restrict the exchanges with the sea and thus limit marine water input in the lagoon

(Mouillot et al., 2000). This lagoon is highly influenced by freshwater inputs from its watershed (182 km^2), and its salinity remains particularly low (Pasqualini et al., 2017). For example, this ranged from 2.0 to 18.5 between November 2013 and December 2014. Freshwater comes from rainfall, sewage plants, several rivers draining the watershed and flowing in the north-west of the lagoon, the Golu River connected to the lagoon by the Fossone channel in the south-western part, and from pumping stations draining the agricultural plain in the southern part of the watershed (Erostate et al., 2018) (Fig. 1). Therefore, Biguglia lagoon displays a salinity gradient from the north to the south (Garrido et al., 2016).

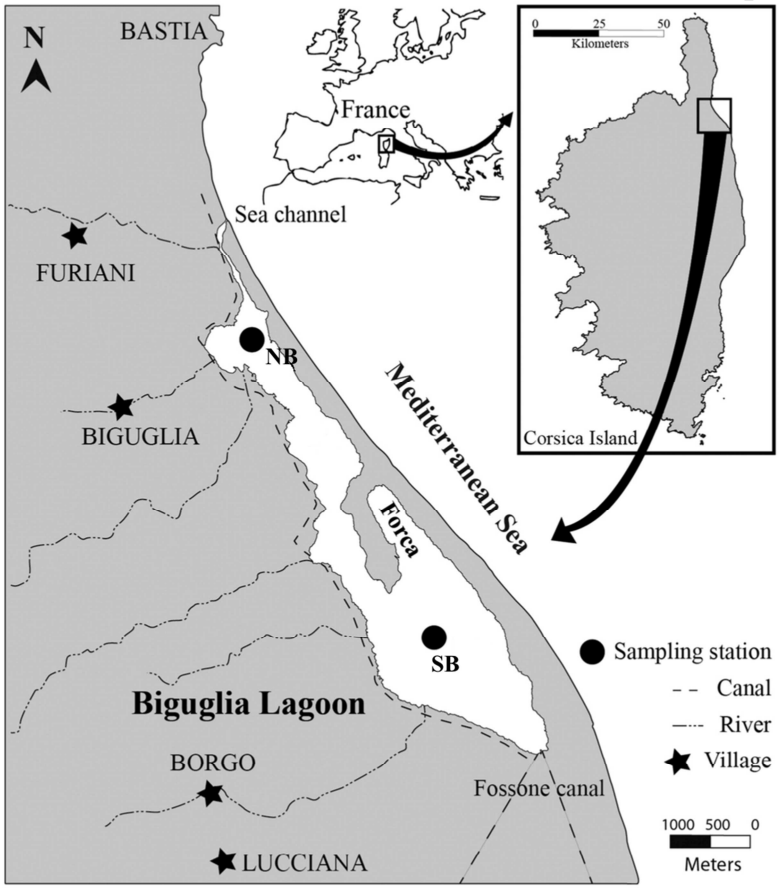

Fig. 1. Location of the two stations representatives of the Northern Basin (NB) and the Southern Basin (SB) of Biguglia lagoon.

Biguglia lagoon has been increasingly eutrophicated since the 1980s due to an intensification of human activities and urbanization on its watershed southward of city of Bastia, including four towns hosting approximately 35,000 inhabitants in winter (Lafabrie et al., 2013). During summer touristic period, the population doubles, which results in increasing anthropogenic pressure. Hence, this lagoon displays very high nutrients concentrations (NH_4^+, NO_2^-, NO_3^-, DIN, Si, TP, TN) in the water column, enhanced by the reduced exchanges with the sea (Orsoni et al., 2001). The sediment compartment shows an important silting with high nutrient concentrations and organic matter content compared to other French Mediterranean coastal lagoons (Souchu et al., 2010). An eutrophication gradient is also observed from the south to the north because of substantial anthropogenic inputs in the southern part of the lagoon.

The lagoon has a Mediterranean climate with a succession of a dry and warm summer and wet autumn, winter and spring seasons with sudden and plentiful rainfalls causing flash floods (Pasqualini et al., 2017). The salinity and nutrients inputs are strongly influenced by theseasonal variability of the climate (Collos et al., 2003). This generally determines three hydrological seasonal periods characterized by differences in their nutrient origin and availability, in phytoplankton biomass and size class structure, and in photosynthetic performance (Cecchi et al., 2016; Garrido et al., 2016).

2.2. *Sampling procedures*

Water samples were collected in two stations representatives of the northern (NB) and the southern (SB) basins (Fig. 1, 42°38'12"N, 9°27'15"E and 42°35'00"N, 9°29'18"E, respectively).

Experiments were carried out in autumn 2013 (26 November to 5 December), spring 2014 (2 to 8 April), and summer 2014 (9 to 12 September). In each of the two NB and SB stations, 70 l of pre-filtered water through 1000 µm mesh to remove larger debris without removing zooplankton or larger phytoplankton cells (Collos et al., 2005) were sampled in sub-surface (20 cm depth) wit a pump from a small boat between 7.00 am and 8.00 am, and kept in the dark. Sub-surface salinity, temperature, percentage of dissolved oxygen (DO) and turbidity were measured *in situ* with a multi parameter Water Quality Probe (YSI® 6600 V2-2). Upon return to the laboratory, water samples were homogenized by gentle shaking, aliquoted and immediately stored at -20°C for the characterization of phytoplankton communities. Measures of NH_4^+, PO_4^{3-}, NO_3^-, NO_2^-, TN, and TP concentrations (µM) were performed on duplicates of 80 ml, filtered on 20 µm meshes for the dissolved inorganic nutrients (Aminot and Chaussepied, 1983).

2.3. *Characterization of phytoplankton biomass*

Chlorophyll *a* (Chl *a*) concentrations (µg l^{-1}) were used as a proxy for phytoplankton biomass. Chl *a* measurements were performed on the total and the fractioned water samples. This allowed assessing the contribution of the ultraphytoplankton <5 µm, the nanophytoplankton between 5 and 20 µm and the microphytoplankton >20 µm to the total biomass. Upon return to the laboratory, triplicates of water samples (maximum 100 ml, depending on phytoplankton abundance) and of samples pre-filtered on 20 µm and on 5 µm meshes were analyzed by spectrofluorimetry (Neveux and Lantoine, 1993). The biomasses of the three size classes were estimated by subtracting the concentrations obtained for the fraction <20 µm to the total water (microphytoplankton), and the fraction <5 µm to the fraction <20 µm (nanophytoplankton). The Chl *a* concentration of the fraction <5 µm estimated the ultraphytoplankton biomass.

217

218 2.4. *Assessment of phytoplankton community composition*

219 Composition and abundance of the ultraphytoplankton <5 µm were studied using flow
220 cytometry. Triplicates of 1 ml of sample fixed with 2 % formaldehyde (filtered on 0.2 µm,
221 final concentration) were submitted to a flash freeze in liquid nitrogen and then stored at -
222 80°C until analysis. Cells counts were performed with a FACSCalibur flow cytometer
223 (Becton Dickinson), using beads for size calibration. Populations of coccoid phycoerythrin-
224 rich picocyanobacteria (PE-cyanos) were identified by light diffraction (FSC) and their
225 orange fluorescence emissions, while phycocyanin-rich picocyanobacteria (PC-cyanos) were
226 distinguished by their low red fluorescence and their absence of orange fluorescence.
227 Photosynthetic picoeukaryotes <3 µm were identified by their red fluorescence emissions
228 (Chl *a*, wavelength >650 nm).

229

230 Optical microscopy was used to describe nano- and microphytoplankton (>5 µm) composition
231 and abundance. Triplicates of 1 l of sample fixed with formaldehyde (5 % final concentration)
232 were stored at obscurity prior to analysis. A modified method of the Utermöhl protocol was
233 used (Leruste et al., 2018). Samples were examined with an optic microscope Olympus
234 AX10. At least 400 cells per sample were counted to obtain a relevant assessment of the
235 assemblage. Taxonomic resolution was realized at species level whenever possible, and
236 identification was verified according to several books (Bellinger and Sigee, 2015; Bérard-
237 Therriault et al., 1999; Loir, 2004; Tomas, 1997) and database such as the World Register of
238 Marine Species (http://www.marinespecies.org/, databases available online). Taxonomic
239 diversity was explored using species richness and Shannon index (Leruste et al., 2018).

240

241 2.5. *Experimental procedure of bioassay experiments*

242 To measure maximal growth rate, five dilutions of water sample (9, 17, 43, 74 and 100 %) in
243 0.2 µm filtered sample in duplicate were incubated with an enrichment containing vitamins,
244 silica, metals trace, nitrogen and phosphorus (NaH_2PO_4, final concentration 0.8 µM) (Landry
245 and Hassett, 1982). Nitrogen was supplied as nitrate and/or ammonium (f/2 and h/2 media,
246 respectively, Guillard & Ryther, 1962) depending on season. In April 2014, N was supplied as
247 nitrate (20 µM final concentration), assuming that nitrate inputs from the watershed were the
248 main nitrogen source. In September 2014, N was supplied as ammonium (20 µM final
249 concentration), assuming that this may be the predominant form provided from
250 remineralization processes in the sediment (Collos et al., 2003). In November-December
251 2013, N was supplied as a mix of nitrate and ammonium (10 µM final concentration each),
252 assuming that sufficiently high temperatures allow the regeneration of ammonium from the
253 sediments, associated with flash floods bringing nitrate from the watershed. This nitrogen
254 concentration has been chosen to avoid phytoplankton growth limitation during the
255 incubation, which has been occasionally observed at 10 µM in another Mediterranean lagoon
256 (Bec et al., 2005). To highlight the potential growth limitation of phytoplankton by N and/or
257 P, two other dilution series were enriched either without nitrogen or phosphorus (Andersen et
258 al., 1991). Two bottles of sample without dilution and enrichment were incubated as control,
259 and the all bottles were simultaneously incubated for 24 h in Biguglia lagoon under *in situ*
260 temperature and light conditions at 30 cm depth.

261

262 2.6. *Estimation of maximal growth rate and N-/P-limitation*

263 After 24 h incubation, the temporal changes of the total and size-fractionated Chlorophyll *a* in
264 each bottle were used to calculate their apparent specific growth rate $k(x)$ for each dilution x.

The relationship between the apparent growth rates $k(x)$ in the fully-enriched bottles and dilution factor x were fitted to the linear equation (1):

$$k(x) = \mu_{max} - gx \quad (1)$$

Where $k(x)$ is the phytoplankton apparent growth rate in the bottles at dilution x, μ_{max} is the maximal growth rate under nutrient replete conditions, and g is the grazing rate. All rates were expressed on a per day basis (d^{-1}). The maximal growth rate μ_{max} was obtained from the Y axis intercept, and the phytoplankton mortality rates g as the slope of the linear regressions assuming that mortality was due to grazing (Landry and Hassett, 1982). Equations were fitted with the 'lmer' function in the 'lme4' library (version 1.1-10, (Bates et al., 2015)) to evaluate if the linear model best fitted the trend of the relationship between the apparent growth rate and the dilution factor. To check whether the linear equation (1) was acceptable, we also considered a quadratic function by adding the term ax^2. The quadratic function has a parabolic pattern and could reflect the contribution of regenerated resources or a saturation of the grazing rate in the less diluted bottles (Andersen et al., 1991). All combinations of the parameters of the quadratic function were considered, and model selection was based on parsimony using the small-sample corrected Akaike's information criterion (AIC_c) (Burnham and Anderson, 2004). Therefore, we calculated the difference between the AIC_c of the linear model and the model having the lowest AIC_c, *i.e*. the most parsimonious model, to obtain a ΔAIC_c value. The models with a ΔAIC_c <2 were considered as having equivalent levels of support (Burnham and Anderson, 2004), using the 'dredge' function of the MuMIn package (Bartón, 2013). Hence for ΔAIC_c <2 we selected the linear model as it allows calculating μ_{max} and g according to equation (1) (Landry and Hassett, 1982), while the quadratic relationship did not allow calculating μ_{max} and g.

289 Phytoplankton net growth rate in controls (μ_0) was calculated by adding g to the apparent
290 growth rate (k_0) *i.e.* $\mu_0 = g + k_0$. Hence, it was assumed that grazing rate was not impacted by
291 nutrient enrichments. The μ_0:μ_{max} ratio assessed the impact of inorganic nutrient enrichment
292 on growth, and estimated the nutrient sufficiency for phytoplankton growth (Landry and
293 Hassett, 1982; Landry et al., 1998).

294

295 In the selectively enriched bioassays, we took account that apparent growth rate is not
296 necessarily a linear function of the dilution factor, because the instantaneous growth rate may
297 decline as internal and external nutrient pools become depleted. μ_{-N} and μ_{-P} were calculated as
298 followed: $\mu_{-N} = g + k_{-N}$ and $\mu_{-P} = g + k_{-P}$. To estimate how much phytoplankton growth was N-
299 and/or P-limited, the ratio between growth rate with the enrichments minus N or minus P (μ_{-N}
300 or μ_{-P}) and maximal growth rate in theoretically non-limiting nutrient condition (μ_{max}) was
301 calculated. Differences between growth rates with full enrichment, enrichment minus N and
302 enrichment minus P helped distinguish different types of co-limitation (Harpole et al., 2011;
303 Burson et al., 2016).

304

305 2.7. *Statistical analyses*

306 Data analysis was performed on R (R Core Team, 2013).

307 Two-way ANOVAs assessed if the total phytoplankton biomass significantly changed among
308 the three samplings and between NB and SB. Posteriori pairwise mean comparisons between
309 stations and samplings were made using Tukey-Kramer's post-hoc analysis (alpha level =
310 0.05). Permanovas assessed if the size class structure varied among stations and samplings,
311 according to differences of biomass, temperature, salinity, dissolved inorganic nutrients, TN
312 and TP concentrations, turbidity and DO (Anderson, 2001). Taxonomic diversity indices *i.e.*
313 the Shannon index on the relative abundance of taxa and morphotypes (H), and the species

314 richness (S) were estimated using Vegan package (Oksanen et al., 2018). ANOVAs assessed
315 if S and H significantly changed among stations and samplings. Spearman's rank correlations
316 between S, H, total Chl *a* biomass and environmental variables (temperature, salinity,
317 inorganic nutrient concentrations, TN and TP concentrations, turbidity and DO) were assessed
318 for the two stations and the three samplings.
319
320 Regression analyses determined which mixed models (*i.e.* combinations of explanatory
321 factors) best fitted the biomass of total phytoplankton and the three size classes. Among all
322 the possible fixed effects (stations, samplings, salinity, temperature, nutrients concentrations,
323 dissolved oxygen, and turbidity), the most relevant were chosen according to a correlation
324 matrix. Values of fixed effects were scaled prior to analysis. Because of pseudo-replication
325 (each triplicate was taken from the same bottle), a random effect was added as a bottle effect.
326 Models were fitted with the 'lmer' function and model selection was assessed using the AIC_c
327 (see below). To estimate the relative importance of each fixed effect, the AIC_c-w of every
328 model was summed (Patiño et al., 2013), and to estimate the variable force effect, we used the
329 mean of the relative coefficient weighted by the AIC_c-w.
330
331 3. Results
332 3.1. *Environmental variables and phytoplankton biomass*
333 Salinities were low during the three dilution experiments, ranging from 2.0 in NB in April, to
334 10.9 in September 2014 (Table 1). The percentage of DO was the lowest in September 2014
335 for both stations, and was negatively correlated with the temperature for the three sampling
336 periods (Table 2, Spearman's rank correlations, *p*-value <0.05). Turbidity was highest in the
337 autumn sampling (Table 1).
338

Concentrations of dissolved inorganic nutrients (NH_4^+, NO_3^-, NO_2^-, DIN, PO_4^{3-}) and of TN and TP were extremely variable. In the sampling in November-December 2013, both stations presented the highest PO_4^{3-} concentrations, and NB displayed the highest concentration of dissolved inorganic nutrients, DIN being mainly composed of NO_3^- (Table 1). In April 2014, N was mainly represented by NO_3^- in the two stations, and N levels were especially high in SB, with 106.5 µM of TN and 95.4 µM of DIN. Inversely, in September 2014, both stations displayed low NO_3^- concentrations (<0.15 µM) and NH_4^+ was the main nitrogen form. TP was higher in SB than in NB in all three samplings (Table 1). All dissolved inorganic nutrient concentrations and TN and TP concentrations were negatively correlated with the temperature. Moreover, NH_4^+ concentrations were also negatively correlated with the salinity. DIN forms were positively correlated between them, and NO_3^- and NO_2^- concentrations were also positively correlated with TN and TP concentrations. PO_4^{3-} concentrations were positively correlated with the percentage of DO (Table 2). The TN:TP and DIN:DIP ratios displayed highest values in April 2014, respectively 71.0 in SB and 124.5 in NB.

The biomass of the total phytoplankton significantly differed among stations and samplings, and the differences among samplings also changed between the two stations (Fig. 2, ANOVA, *p*-value <0.05). Chlorophyll *a* (Chl *a*) concentration generally ranged between 3.5 and 6.0 µg l^{-1}, with the exception in SB in December 2013 when it peaked at 20.6 µg l^{-1} (Fig. 2A). Taking all samplings collectively, we found that Chl *a* concentration showed a negative relationship with the salinity and NH_4^+ concentrations, the latter effect changing among stations (Regression analyses, force of the salinity effect: -4.5, and of the NH_4^+ concentration: -8.1). Total biomass was significantly higher (i) in SB than in NB, (ii) in the autumn sampling than in April and in September 2014, as well as (iii) in April than in September samplings (Fig. 2, pairwise Tukey multiple comparisons, p <0.05). The total biomass was negatively correlated

364 with temperature, and positively correlated with NO_2^-, NO_3^-, PO_4^{3-} concentrations and with
365 the percentage of DO, reflecting the peak of biomass observed in December in SB (Table 2,
366 Spearman's rank correlations, *p*-value <0.05).

Table 1. Mean values of environmental parameters in the two NB and SB stations of Biguglia lagoon in November-December 2013, April and September 2014. DO: dissolved oxygen. Dissolved inorganic nitrogen is expressed as DIN = NH_4 + NO_3 + NO_2. Dissolved inorganic phosphorus corresponds to PO_4^{3-} concentration.

Sampling periods	Stations	Date	T°(C)	Salinity	DO (%)	Turbidity (NTU)	TN	NH_4^+	NO_3^-	NO_2^-	DIN	TP	PO_4^{3-}	TN:TP	DIN:DIP
							(µM)								
Nov -Dec 2013	NB	26/11/13	8.3	4.7	100.8	2.87	84.37	7.52	70.01	0.49	78.03	1.37	0.73	61.4	107.3
	SB	04/12/13	8.2	6.1	101.5	16.83	61.87	0.69	40.72	0.29	41.70	1.77	0.64	34.9	65.5
April 2014	NB	07/04/14	15.0	2.0	113.0	0.80	34.55	2.18	17.47	0.16	19.80	0.82	0.16	41.9	124.5
	SB	02/04/14	15.5	6.0	93.2	4.63	106.47	1.85	93.22	0.30	95.38	1.50	0.00	71.0	-
September 2014	NB	11/09/14	24.8	10.9	97.0	1.83	38.51	0.37	0.03	0.00	0.40	0.89	0.03	43.3	13.3
	SB	09/09/14	25.9	6.0	86.2	10.50	29.95	1.24	0.11	0.09	1.44	1.17	0.11	25.6	13.1

Table 2. Spearman's rank correlation between species richness (S), Shannon index (H), Chl *a* concentrations and environmental variables at the 95% confidence interval for the three sampling periods in both NB and SB stations of Biguglia lagoon. Significant correlations are in bold. DO: dissolved oxygen. ****p*-value <0.001, ***p*-value <0.01, **p*-value <0.05.

	S	H	Chl *a*	Temperature	Salinity	NH_4^+	NO_2^-	NO_3^-	PO_4^{3-}	TN	TP	Turbidity
H	-0.314											
Chl *a*	-0.312	**0.626****										
Temperature	**0.469***	**-0.661****	**-0.900*****									
Salinity	-0.051	**-0.693****	-0.242	0.203								
NH_4^+	-0.066	**0.680****	0.260	-0.314	**-0.928*****							
NO_2^-	**-0.513***	**0.536***	**0.530***	**-0.657****	-0.464	**0.714*****						
NO_3^-	**-0.494***	0.335	**0.492***	**-0.543***	-0.377	**0.600****	**0.943*****					
PO_4^{3-}	-0.405	**0.836*****	**0.709*****	**-0.880*****	-0.400	**0.516***	**0.637****	0.395				
TN	-0.280	-0.009	0.360	**-0.486***	0.058	0.257	**0.771*****	**0.829*****	0.273			
TP	**-0.809*****	0.047	0.398	**-0.486***	0.319	-0.086	**0.600****	**0.657***	0.273	**0.657****		
Turbidity	**-0.828*****	-0.041	0.122	0.143	0.406	-0.314	0.200	0.257	0.030	0.143	**0.829*****	
DO	0.041	**0.624****	**0.774*****	**-0.771*****	-0.348	0.257	0.200	0.086	**0.698****	0.029	-0.143	-0.371

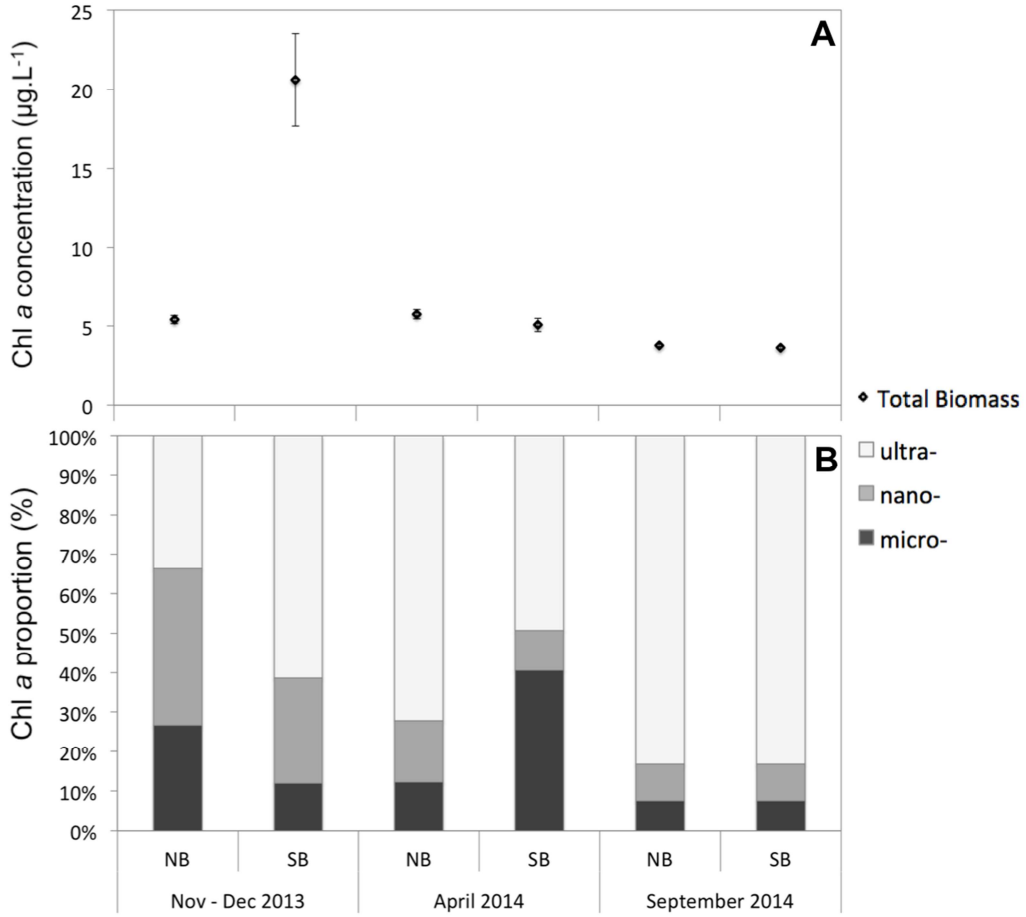

Fig. 2. Mean chlorophyll *a* (Chl *a)* concentration (µg l^{-1}) (A) in the three samplings at the NB and SB stations in Biguglia lagoon. Error bar indicates standard deviations. Proportions of the different size classes of phytoplankton contributing to phytoplankton biomass (B), *i.e.* microphytoplankton >20 µm (dark grey), nanophytoplankton between 5 and 20 µm (grey) and ultraphytoplankton <5 µm (light grey).

3.1. *Phytoplankton community composition*

The size class structuration of phytoplankton communities was significantly different between the NB and SB stations among the three samplings (Fig. 2B), and the differences between samplings changed between stations (Permanova, *p*-value <0.05). Taking all samplings collectively, the ultra- and the nanophytoplankton biomasses showed a positive relationship with the salinity and the phosphorus concentrations. In contrast, the microphytoplankton biomasses showed a positive relationship with NO_3^- concentrations and a negative

388 relationship with NH_4^+ concentrations (Regression analyses, delta-AICc <2).
389 Ultraphytoplankton was the major group in the phytoplankton communities (up to 87 % of
390 Chl *a* in September 2014) (Fig. 2B), except for NB in November 2013, when a higher
391 proportion of nanophytoplankton (40 %) than ultraphytoplankton (34 %) was observed. For
392 both stations, the nanophytoplankton biomass was highest in November 2013.

393

394 The taxonomic diversity indices showed different patterns at the two stations and among the
395 three samplings. Both the species richness (S) and the Shannon index (H) significantly
396 changed among stations and samplings (ANOVAs, both *p*-values <0.05). S was the lowest in
397 the autumn sampling and highest in the sampling in September for the two stations, while H
398 showed the inverse trend. Hence, S was positively correlated with temperature, and negatively
399 correlated with NO_2^-, NO_3^-, TP concentrations and turbidity (Table 2). H was positively
400 correlated with total biomass, NH_4^+, NO_2^- and PO_4^{3-} concentrations and percentage of DO,
401 while it was negatively correlated with temperature and salinity (Table 2).

402

403 Fig. 3 gives the contributions of four size classes (<3 µm, between 3 and 5 µm, between 5 and
404 20 µm and >20 µm) to the total abundances of cell counts in the two stations at the three
405 sampling periods, and Fig. 4 specifies the main taxonomic classes represented in each of the
406 size classes. For the three samplings, small cells dominated the phytoplankton communities
407 (Fig. 3). The NB station showed higher Bacillariophyceae abundances than SB, while the SB
408 station showed higher Chlorophyta and Cryptophyceae abundances (Fig. 4). NB has also
409 displayed higher dinoflagellates abundances than SB, except in November-December 2013
410 (Fig. 4).

411

In the sampling in November 2013, the phytoplankton community in NB showed a bloom of the dictyochophycean *Apedinella radians* (Lohmann) P.H. Campbell, 1973 (1.3 x 10^6 cells.l^{-1}, *i.e.* 41.6 % of total abundances, Fig. 3-4). This community also comprised high abundances of eukaryotes with flagella between 3 and 5 µm (6.9 x 10^5 cells.l^{-1}, Fig. 3-4), and of *Prorocentrum cordatum* (Ostenfeld) J.D.Dodge, 1975 *alias Prorocentrum minimum* (Pavillard, 1916) J.Schiller, 1933 (2.9 x 10^5 cells.l^{-1}, Fig. 4). Dinoflagellates dominated the community in SB in December, mainly represented by *Heterocapsa minima* Pomroy, 1989 (5.1 x 10^6, *i.e.* 34.2 % of total abundances Fig. 3), associated with *A. radians* (4.8 x 10^6 cells.l^{-1}, Fig. 4). Microphytoplanktonic cells were scarce (*e.g. Kryptoperidinium foliaceum* Lindemann, 1924: 3.7 x 10^3 cells.l^{-1}; *Cocconeis* sp.: 3.7 x 10^3 cells.l^{-1}; *Prorocentrum micans* Ehrenberg 1834: 1.5 x 10^3 cells.l^{-1}). Conversely, we observed a bloom of *Mesodinium rubrum* Lohmann, 1908 (2.3 x 10^5 cells.l^{-1}, *i.e.* 78 % of the microplanktonic cells, Fig. 4).

In the sampling in April 2014, dinoflagellates dominated the NB community mainly due to a bloom of *H. minima* (3.7 x 10^6 cells.l^{-1}, *i.e.* 35.8 % of total abundances, Fig. 3-4). Bacillariophyceae were also abundant and distributed among the three size classes >3 µm (3.1 x 10^6 cells.l^{-1}, Fig. 4) with *e.g. Thalassiosira* sp., *Diatoma* sp., and *Chaetoceros* spp.. The SB community was dominated by phycocyanin-rich picocyanobacteria (PC-cyanos, 6.4 x 10^7 cells.l^{-1}, *i.e.* 49.6 % of total abundances, Fig. 3-4), Picoeukaryotes (Peuk) without flagella (5.6 x 10^7 cells.l^{-1}) and eukaryotes with flagella between 3 and 5 µm (5.9 x 10^6 cells.l^{-1}, Fig. 4). The two latest morphotypes probably belonged to the green algae according to the pigment composition (data not shown). *M. rubrum* also bloomed as in December 2013 (1.6 x 10^5 cells.l^{-1}, Fig. 4).

436 In the sampling in September 2014 the communities of the two stations were dominated by
437 PC-cyanos (9.4 x 10^8 cells.l^{-1}, *i.e.* 92.7 % of total abundances in NB, 3.0 x 10^8 cells.l^{-1} *i.e.*
438 91.9 % of total abundances in SB, Fig. 3-4) and Peuk without flagella (6.5 x 10^7 cells.l^{-1} in
439 NB, 1.7 x 10^7 cells.l^{-1} in SB, Fig. 3-4), that most likely belonged to the green algae according
440 to the pigment composition (data not shown). The nanophytoplankton in NB displayed high
441 abundances of *Tetraselmis* sp. (2.0 x 10^5 cells.l^{-1}), *P. cordatum* (8.2 x 10^4 cells.l^{-1}) and *H.*
442 *minima* (3.2 x 10^4 cells.l^{-1}). Dinoflagellates dominated the microphytoplankton with
443 *Prorocentrum* sp. *cf mexicanum* Osorio-Tafall, 1942, and *Gonyaulax* sp. (10^4 cells.l^{-1}). We
444 also observed high abundances of *Chaetoceros* spp., and *Ceratoneis closterium* Ehrenberg,
445 1839 (10^4 cells.l^{-1}). The ultra- and the nanophytoplankton in SB also contained high
446 abundances of *A. radians* (1.6 x 10^6 cells.l^{-1}), *Pyramimonas sp.* (8.9 x 10^5 cells.l^{-1}),
447 *Plagioselmis* sp., *H. minima*, *P. minimum* and nanoplanktonic centric diatoms (10^4 cells.l^{-1}).
448 *C. closterium*, and *Gonyaulax* sp. *cf spinifera* (10^4 cells.l^{-1}) were the most abundant
449 microplanktonic cells in SB (Fig. 4).

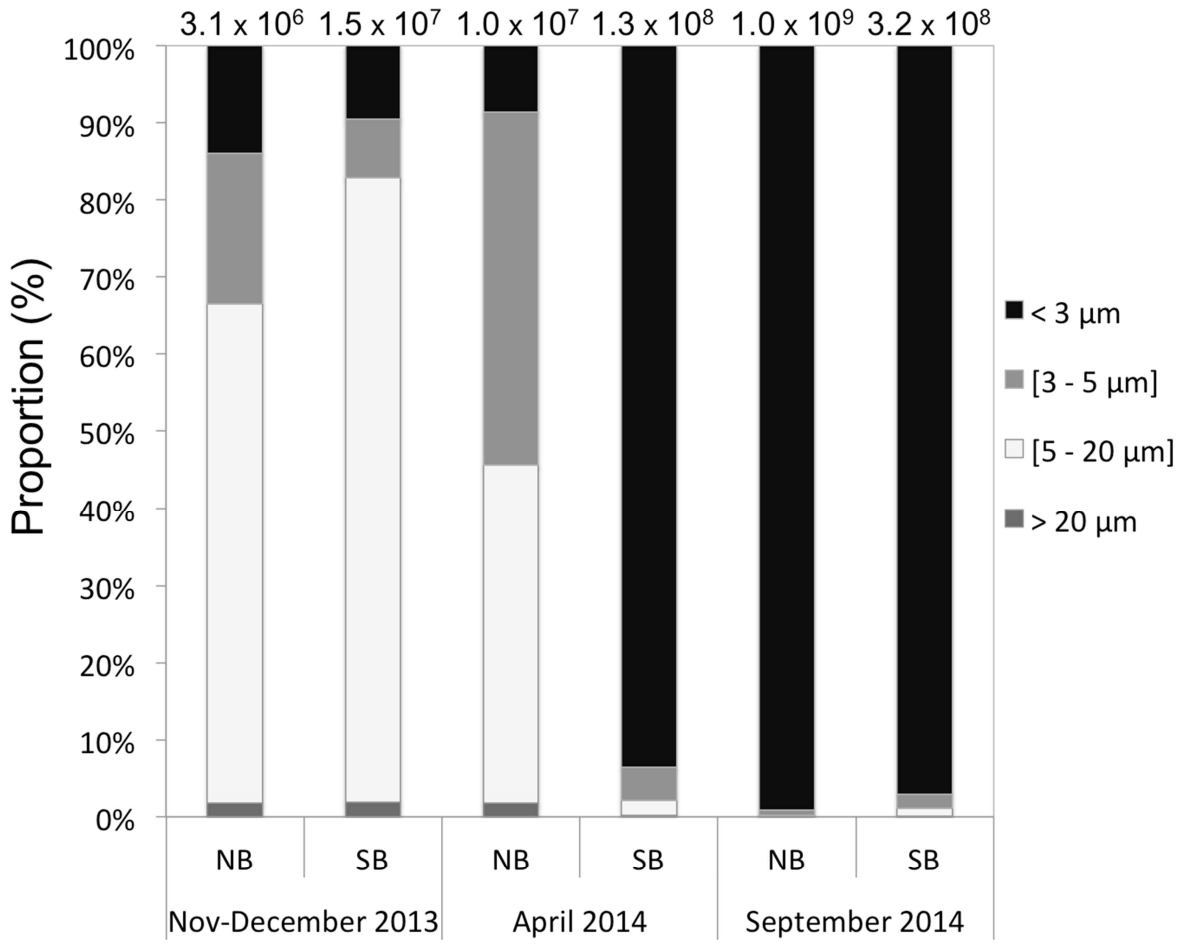

450

451 Fig. 3. Contribution of the size classes <3 µm, [3-5 µm], [5-20 µm] and >20 µm to the total
452 abundances of cell counts in the two NB and SB of Biguglia lagoon at the three sampling
453 periods. Total abundances are specified on the top of the bars.

454

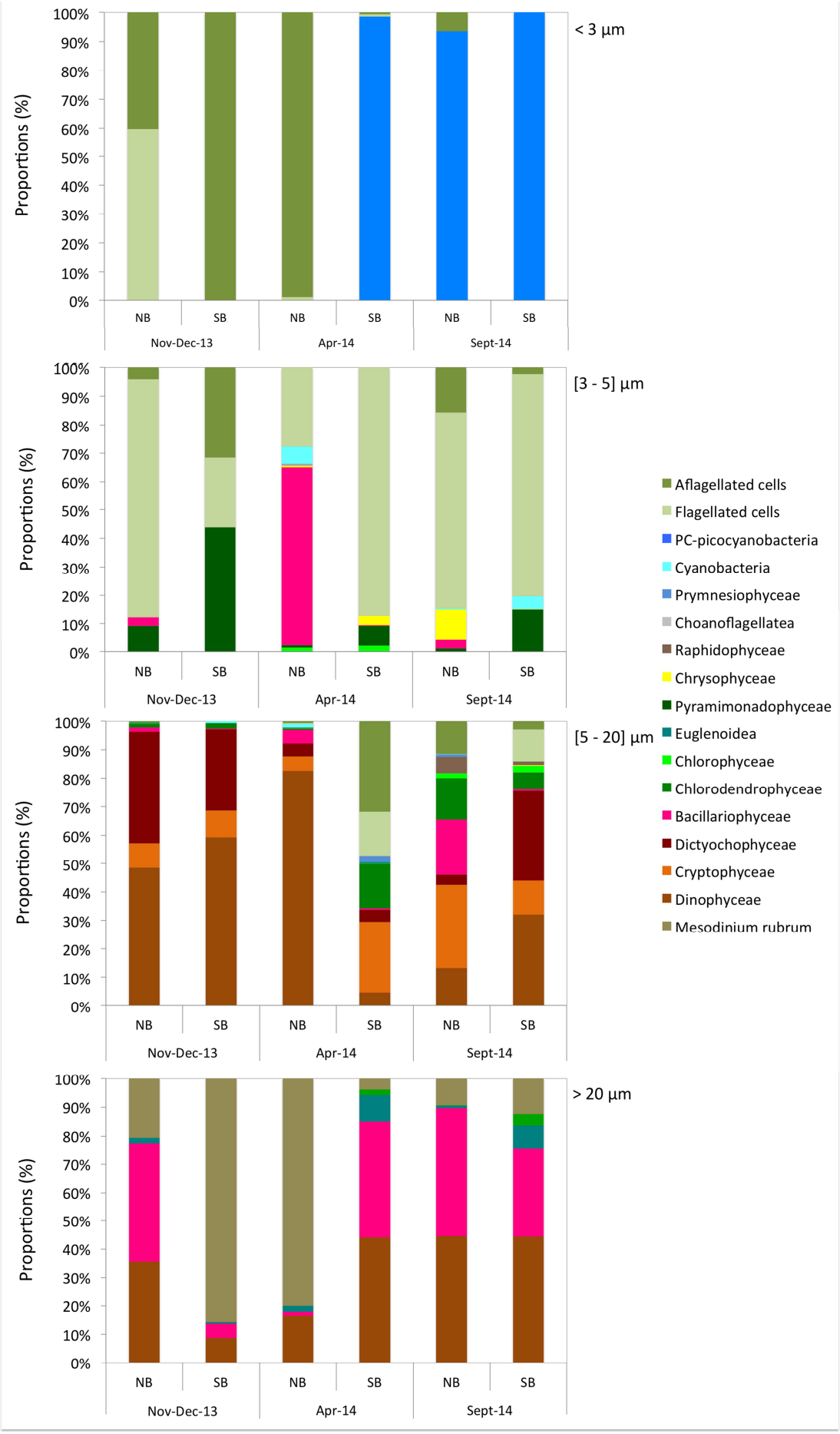
< 3 µm
[3 - 5] µm
[5 - 20] µm
> 20 µm
Proportions (%)
100%
90%
80%
70%
60%
50%
40%
30%
20%
10%
0%
NB
SB
Nov-Dec-13
Apr-14
Sept-14
Aflagellated cells
Flagellated cells
PC-picocyanobacteria
Cyanobacteria
Prymnesiophyceae
Choanoflagellatea
Raphidophyceae
Chrysophyceae
Pyramimonadophyceae
Euglenoidea
Chlorophyceae
Chlorodendrophyceae
Bacillariophyceae
Dictyochophyceae
Cryptophyceae
Dinophyceae
Mesodinium rubrum

455

Fig. 4. Contribution of the main taxonomic classes to the abundances of the four size classes <3 µm, [3-5 µm], [5-20 µm] and >20 µm in the two stations of Biguglia lagoon at the three sampling periods.

3.2. *Phytoplankton net growth and mortality rates without enrichment*

Phytoplankton net growth rates (μ_0) without enrichment ranged from negative values for the microphytoplankton of NB in November 2013 and April 2014, to 1.91 d^{-1} for the nanophytoplankton of SB in April 2014 (Table 3). In November-December 2013, the total phytoplankton displayed low net growth rates (0.45 d^{-1} in NB and 0.48 d^{-1} in SB), and similar mortality rates (0.62 d^{-1} in NB to 0.69 d^{-1} in SB). In NB the ultraphytoplankton dominated by picoeukaryotes (Peuk) displayed a two-fold higher growth rate, while its mortality rate was three times higher than those of the total phytoplankton (Table 3). The nanophytoplankton, mainly comprising *A. radians* and *P. cordatum*, and particularly the microphytoplankton comprising diatoms and dinoflagellates species, showed a loss of biomass after 24 h incubation (Table 3). In SB, only the net growth rate (μ_0) of ultraphytoplankton could have been estimated, but this size class dominated by Peuk has shown a loss of biomass after the 24 h incubation (Table 3, Fig. S2A).

In April, we were able to calculate the μ_0 only for the nanophytoplankton (Table 3, Fig. S2B). In NB, this size class dominated by *H. minima* displayed a high net growth rate (μ_0 = 1.13 d^{-1}) and a relatively low mortality rate (0.28 d^{-1}), while in SB, it was dominated by Chlorophyta and Cryptophyta cells, which displayed the highest estimated μ_0 (1.91 d^{-1}) and a high mortality rate (0.83 d^{-1}).

In September, the net growth rates in NB ranged between 0.50 d^{-1} for the ultraphytoplankton dominated by PC-cyanos and 1.84 d^{-1} for the microphytoplankton dominated by dinoflagellates and Bacillariophyceae. The nano-, dominated by *Plagioselmis* sp., *Tetraselmis* sp., *and P. cordatum*, and the microphytoplankton showed the highest growth rates (μ_0 = 1.6 and μ_0 = 1.8 d^{-1}, respectively) with similar mortality rates (g = 0.57 d^{-1}). In SB, the total phytoplankton and the ultraphytoplankton also dominated by PC-cyanos experienced a loss of biomass after 24 h incubation (Table 3). The nanophytoplankton dominated by *A. radians* and *Plagioselmis* sp. displayed high growth and mortality rates (μ_0 = 1.4 d^{-1}; g = 1.1 d^{-1}). The biomass of microphytoplankton at T0 was too low to estimate their apparent growth rate, we were not able to truly calculate its specific growth and mortality rates.

Table 3. Net growth rate without enrichment (μ_0) and maximal growth rates, with (i) full enrichment (μ_{max}), (ii) enrichment minus N (μ_{-N}), (iii) enrichment minus P (μ_{-P}) for the NB and SB stations of Biguglia lagoon in November-December 2013, April and September 2014. g represents the mortality rate. Bold values specify when the relationship between apparent growth rate as a function of the dilution factor can be explained as a linear model, although for the minus N and minus P enrichments other models can also fit this relationship; the μ_0:μ_{max} ratio illustrates the impact of the full enrichment on phytoplankton growth; the ratios between growth rates with selectively N- or P-enrichment (μ_{-N} or μ_{-P}) and μ_{max} highlight N- or P-limitations (μ_{-X} :μ_{max} = 1 no limitation, μ_{-X} :μ_{max} <1 limitation of the lacking nutrient X, μ_{-X} :μ_{max} >1 limitation of the added nutrient).

Stations	Samplings	Fraction	μ_0	g	μ_{max}	μ_0:μ_{max}	μ_{-N}	μ_{-N} :μ_{max}	μ_{-P}	μ_{-P} :μ_{max}
				(d^{-1})			(d^{-1})		(d^{-1})	
NB	Nov - Dec 2013	Total	**0.45**	**0.62**	**<0**	-	**<0**	-	**0.30**	<0
		Micro-	<0	1.45	<0	-	<0	-	<0	-
		Nano-	0.37	0.26	0.46	0.79	**0.62**	1.34	**1.13**	2.44
		Ultra-	**0.96**	**1.82**	**<0**	-	**<0**	-	<0	-
	April 2014	Total	<0	<0	0.25	-	**0.51**	1.99	**0.07**	0.29
		Micro-	<0	1.01	0.24	-	1.59	6.70	1.01	4.24
		Nano-	**1.13**	**0.28**	**1.83**	**0.62**	1.95	1.06	1.54	0.84
		Ultra-	<0	0.43	<0	-	<0	-	<0	-
	September 2014	Total	**0.64**	**0.30**	**1.78**	**0.36**	0.86	0.48	1.03	0.58

		Micro-	**1.84**	**0.57**	**3.40**	**0.54**	**1.78**	0.52	**2.24**	0.66
		Nano-	**1.60**	**0.57**	**2.70**	**0.59**	1.77	0.65	**2.13**	0.79
		Ultra-	**0.51**	**0.45**	**1.12**	**0.45**	**0.51**	0.46	**0.52**	0.46
SB	Nov - Dec 2013	Total	**0.48**	**0.69**	**0.41**	**1.19**	0.26	0.64	**0.53**	1.31
		Micro-	1.12	1.12	0.45	2.48	1.09	2.41	1.05	2.32
		Nano-	1.17	0.50	0.90	1.30	0.78	0.87	**1.07**	1.19
		Ultra-	**<0**	**1.10**	**0.14**	**<0**	**1.85**	13.68	**2.02**	14.94
	April 2014	Total	0.17	<0	0.19	0.92	0.06	0.31	**0.26**	1.35
		Micro-	-	-	-	-	-	-	-	-
		Nano-	**1.91**	**0.83**	**2.00**	**0.95**	1.64	0.82	**1.64**	0.82
		Ultra-	<0	<0	0.01	<0	**0.10**	8.73	**0.34**	27.96
	September 2014	Total	**<0**	**0.16**	**1.79**	**<0**	0.28	0.16	1.34	0.75
		Micro-	-	-	-	-	-	-	-	-
		Nano-	**1.42**	**1.14**	**3.23**	**0.44**	**1.58**	0.48	<0	<0
		Ultra-	**<0**	**<0**	**0.87**	**<0**	**<0**	<0	<0	<0

3.3. *Bioassay experiments*

In November and December 2013, the full enrichment including NO_3^-, NH_4^+ and PO_4^{3-} did not enhance phytoplankton growth rates in the two stations. The total phytoplankton, the micro- and ultraphytoplankton in NB experienced a loss of biomass after 24 h incubation compared with the controls. Only the growth rate of the ultraphytoplankton of SB was higher with the enrichment, and showed a linear relationship between the apparent growth rate and the dilution factor. This indicates a nutrient limitation for this class size (Table 3). In NB, the enrichment minus N has only resulted in a higher growth rate of the nanophytoplankton. The non-linear relationship between the apparent growth rate and the dilution factor for the ultraphytoplankton (Fig. S2A) suggests the use of other resources than the externally supplied nutrients, or a saturation of predation in the less diluted samples. The enrichment minus P partly released the total phytoplankton growth from N-limitation, allowing a positive growth rate. Ratios between μ_{-N} *or* μ_{-P} *and* μ_{max} for the nanophytoplankton indicate an independent co-limitation by N and P. The negative growth rates of the micro- and ultraphytoplankton, and the non-linear relationship between their apparent growth rate and the dilution factor with the enrichments minus N and minus P more likely suggest a co-limitation by N and P (Table 3,

518 Fig. S2A). In SB, ratios between μ_{-N} *or* μ_{-P} *and* μ_{max} of the total phytoplankton and of the
519 nanophytoplankton, as well as their non-linear relationship between apparent growth rates and
520 dilution factors suggest a single N-limitation (Table 3, Fig. S2B). The higher growth rate of
521 microphytoplankton with the enrichments minus N and minus P compared with μ_{max} (Table 3)
522 suggests a co-limitation by N and P. Ratios between μ_{-N} *or* μ_{-P} *and* μ_{max} for the
523 ultraphytoplankton suggest an independent co-limitation by N and P (Table 3).

524

525 In April 2014, the full enrichment with NO_3^- and PO_4^{3-} resulted in an increase of the growth
526 rate of the nanophytoplankton by 62 % and 5 % in NB and SB respectively. The non-linear
527 relationship between the apparent growth rate and the dilution factor indicates that other
528 fractions in the two stations may have been limited despite the full nutrient enrichment (Table
529 3, Fig. S3). In NB, ratios between μ_{-N} *or* μ_{-P} *and* μ_{max} of the total phytoplankton and of the
530 nanophytoplankton suggest a single P-limitation. The microphytoplankton displayed an
531 independent co-limitation of N and P, which was more pronounced for P. The negative μ_{-N}
532 and μ_{-P} of the ultraphytoplankton, and the relationship between their apparent growth rate and
533 the dilution factor in the enrichments minus N and minus P also suggest a co-limitation by N
534 and P (Table 3, Fig. S3A). In SB, ratios between μ_{-N} *or* μ_{-P} *and* μ_{max} of the total phytoplankton
535 indicate a single N-limitation, while those of the nano- and of the ultraphytoplankton indicate
536 a simultaneous and an independent co-limitation by N and P respectively (Table 3, Fig. S3).
537 This is also supported by the non-linear relationship between their apparent growth rate and
538 the dilution factor that may highlight the use of other N and P resources to cope with the
539 nutrient limitation (Table 3, Fig. S3B).

540

541 In September 2014, the enrichment with NH_4^+ and PO_4^{3-} led to more than the doubling of the
542 growth rate of most of phytoplankton size classes in NB (Table 3), indicating a strong nutrient

limitation. The microphytoplankton of NB displayed the highest μ_{max} of the two communities for the three bioassays. In SB, the full enrichment has allowed a release from nutrient limitation of the entire community, especially for the ultraphytoplankton and the nanophytoplankton (Table 3). In NB, ratios between μ_{-N} *or* μ_{-P} *and* μ_{max} of the total phytoplankton and the three size classes suggest a N and P co-limitation, that was serial for the micro- and for the ultraphytoplankton, and independent for the nanophytoplankton (Table 3). In SB, ratios between μ_{-N} *or* μ_{-P} *and* μ_{max} of the three size classes indicate an independent co-limitation by N and P for the total phytoplankton, a serial co-limitation by N and P for the nanophytoplankton and a simultaneous co-limitation by N and P for the ultraphytoplankton (Table 3, Fig. S4B).

4. Discussion

In this study, we aimed to describe functional traits of phytoplankton communities in Biguglia lagoon submitted to a strong anthropogenic impact in different seasons with contrasting environmental conditions, and the response of these communities to various forms of nutrients inputs simulating nutrient pulses to predict their impact on ecosystem functioning.

4.1. *Functional traits of phytoplankton communities in response to environmental conditions*

Biguglia lagoon was globally strongly influenced by freshwater inputs from the watershed and from the connection with one of the main river in Corsica in the south of the lagoon. These freshwater inputs have contributed to maintain a low salinity that prevailed in the two sub-basins during the year 2014, despite their distinct hydrological dynamics. This freshwater influence has led to the dominance of species associated with brackish or fresh waters in phytoplankton assemblages. Phycocyanin-rich picocyanobacteria (PC-cyanos) and flagellates

568 from the Dictyochophyceae, dinoflagellates, Chlorophytes, and Cryptophytes were the main
569 representative groups in the two stations at the three samplings. Their size structure,
570 community composition and productivity illustrate their functional responses to lagoon
571 variability.
572
573 Biguglia lagoon was principally enriched by high nitrogen inputs, especially during the wet
574 periods. Indeed, high nitrate inputs from a huge historical accumulation are carried to the
575 lagoon by groundwater flows during strong episodic rainfall events (Erostate et al., 2018).
576 The negative correlations, both between temperature and nutrient concentrations, and between
577 salinity and ammonium concentration also support that freshwater discharge was the main
578 source for nutrient enrichment in the lagoon at the three sampling periods (Garrido et al.,
579 2016; Pasqualini et al., 2017). The important precipitations in November 2013 and Marsh
580 2014 (150.4 mm and 92.6 mm respectively, https://www.infoclimat.fr/, Station of Bastia
581 Poretta) explain the high NO_3^- concentrations and high TN:TP and DIN:DIP values in the
582 autumn and spring samplings. In contrast, low dissolved inorganic nitrogen and phosphorus
583 concentrations were observed in September, although the summer period corresponds to the
584 most important period for the recycling of ammonium and phosphate in the lagoon (Collos et
585 al., 2003).
586
587 Phytoplankton cell size decreased with the decrease of DIN availability, which may be
588 explained by higher uptake affinities of small cells under nutrient-limiting conditions
589 (Litchman et al., 2007). High nanophytoplankton biomasses in Biguglia lagoon have already
590 been related to the availability of oxidized forms of nitrogen (Cecchi et al., 2016). In this
591 study, ultra- and nanophytoplankton biomasses were rather positively related to PO_4^{3-}
592 availability. Dominance of fast-growing pico- and nanoflagellates can be frequent in shallow

lagoons exposed to high nutrient loads and submitted to continuous inputs of freshwater or discontinuous floods. These nutrient loads allow the release of the limitation of cells >3 µm that can coexist with fast growing and highly competitive picoeukaryotes (Bec et al., 2011; Coelho et al., 2015).

Nanoplanktonic dinoflagellates were particularly abundant during the samplings in the wet seasons (autumn and spring). We particularly observed blooms (>10^5 cells.l^{-1}) of *P. cordatum* in NB in November 2013, and of *H. minima* in SB in December 2013 and in NB in April 2014. Blooms of *P. cordatum* are frequently related to high N:P ratios in coastal transitional ecosystems characterized by brackish waters (Johnson, 2015), and to freshwater inflows that cause low salinities and high nitrate concentrations (Heil et al., 2005; Coelho et al., 2007; Cecchi et al., 2016). Moreover, *P. cordatum* and some *Heterocaspa* species have demonstrated potential mixotrophic abilities, especially under N- or P-starvation (Legrand et al., 1998; Jeong et al., 2005; Johnson, 2015). The presence of potential preys such as picocyanobacteria, Cryptophytes and small diatoms may thus have stimulated their development despite the potential nutrient limitation.

Biomass of the microphytoplankton, mainly composed of Bacillariophyceae and dinoflagellates in the three samplings, has been positively related to the high NO_3^- concentrations. Indeed, pulses of NO_3^- especially favor fast-growing diatoms during spring blooms in river-dominated coastal ecosystems (Paerl et al., 2010; Donald et al., 2011; Glibert et al., 2015). They were generally most abundant in the northern basin, probably due to their resistance to turbulent environments, their high affinity for nitrate, and the high freshwater inputs (Garrido et al., 2016).

Picophytoplankton (picocyanobacteria and picoeukaryotes) often represents an important component of phytoplankton communities in brackish lagoons. Particularly, phycocyanin-rich picocyanobacteria have shown blooms after floods when salinities achieved their minimal values (Bec et al., 2011; Lafabrie et al., 2013). Small cells have physiological advantages that confer them a high competitiveness to acquire and use nutrients under limiting conditions (Raven, 1998). They are especially competitive in warmer waters and under low N-availability as observed during the summer period (Bec et al., 2005; Leruste et al., 2016; Domingues et al., 2017). Moreover, they are able to use nitrate, ammonium as well as organic N-sources in a highly efficient way (Domingues et al., 2011), and are hardly inhibited by occasionally occurring high ammonium concentrations (Collos and Harrison, 2014). Bloom of picophytoplankton in summer coincides with high regeneration process, and a dominance of ammonium that picophytoplankton can preferentially use, while diatoms and dinoflagellates preferentially use NO_3^-, and are able to show high growth rate in nitrate-rich waters (Domingues et al., 2011; Glibert et al., 2015; Reed et al., 2016).

These competitive trade-offs may thus explain the competitive exclusion of the larger cells by the PC-cyanos in September. Shift between diatoms and dinoflagellates to picophytoplankton from spring to late summer frequently occur in coastal aquatic systems with the shift of available N forms, from NO_3^- (>88% of the DIN in the two stations in November-December 2013 and April 2014) to NH_4^+ (>85 % of the DIN in the two stations in September 2014) (Glibert et al., 2015; Domingues et al., 2017). However, ambient nutrient concentrations are measures of the residual nutrients after biogeochemical activity, and may not reflect the real available nutrient concentrations for phytoplankton growth. The bioassay experiments gave further insights about the relationship between their functional responses to the nutrient

availability. This especially specified which nutrient was potentially limiting for phytoplankton growth at the three sampling periods.

4.2. *Phytoplankton behavior under induced nutrient limitation*

Temperate coastal ecosystems generally display seasonal changes of nutrient availability and limitation, characterized by shifts from a P-limitation during the wet seasons after high nitrate-rich freshwater inputs, to N-limitation during the dry season (Lomas and Glibert, 2000; Kemp et al., 2005). In contrast, we did not observe this pattern in Biguglia lagoon, despite the high DIN inputs from the watershed during the wet seasons, reflected by high TN:TP and DIN:DIP^{-} values. The results of the bioassay experiments more often show a co-limitation by N and P for the phytoplankton communities. Nevertheless, some size fractions were limited by one of these elements alone, *e.g.* the nanophytoplankton of the NB station limited by P in April 2014, and the microphytoplankton of the SB station limited by N in December 2013. A review showed that co-limitation by N and P in freshwater and marine ecosystems is more common than previously thought (Elser et al., 2007). Interestingly, the single limitation for some size fractions within a co-limited community, such as observed in SB in September 2014 may indicate niche differentiation. We also observed that the phytoplankton in SB was more often N-limited than in NB despite high DIN:DIP ratios. Conclusions from the dilution experiment should be drawn with caution, because incubations have been conducted on small spatial and temporal scales. The responses of phytoplankton communities at these scales can differ from the overall ecology of the entire ecosystem (Piehler et al., 2004; Reed et al., 2016). However, these results support that ambient nutrient ratios do not necessarily reflect the availability of nutrients for autotrophic communities, particularly because of the known variability of nutrient stoichiometry of phytoplankton. The communities of the two stations showed the strongest simultaneous or serial co-limitation by N and P in summer while in the

667 wet seasons they showed single N- or P-limitations or independent co-limitation depending on
668 fractions. The figure 5 conceptualizes our observations for the three samplings, and links the
669 environmental specificities, the differences in community structure and composition, with the
670 calculated growth rates and the observed N- and P-limitation.
671
672 Picocyanobacteria, dinoflagellates and other phytoplankton groups have demonstrated
673 numerous ways to acclimate to temporally and varying N- and P-limitation (Lin et al., 2015).
674 For example, luxury PO_4^{3-} uptake prior to sampling for the bioassays could have provided the
675 necessary intracellular P for phytoplankton growth during the 24 h incubation.
676 Picocyanobacteria may have used high P-storage abilities that could have allowed them to
677 maintain their bloom despite low P-availability (Sorokin and Dallocchio, 2008). Moreover,
678 they have shown high inorganic P-uptake efficiency at low levels of available soluble reactive
679 phosphorus (Collos et al., 2009). Alternatively, the high dissolved and particulate organic N
680 and P stocks in the sediment of Biguglia lagoon may have been used by the phytoplankton to
681 thrive despite low dissolved inorganic N- and P-availability. Indeed, the very low dissolved
682 inorganic phosphorus concentrations at the three samplings may have stimulated the
683 production of alkaline phosphatase, allowing the use of dissolved organic phosphorus (Piehler
684 et al., 2004; Lin et al., 2015). Moreover, high abundances of potentially mixotrophic species
685 among *Prorocentrum*, *Heterocapsa*, *Gonyaulax* and other genera, and of *Mesodinium rubrum*
686 (Collos et al., 2014; Fischer et al., 2016; Johnson, 2015) have been observed during these
687 experiments. Mixotrophy is an advantageous behavioral response under nutrient limiting
688 conditions, allowing cells to reduce direct competition for inorganic nutrients (Jeong et al.,
689 2005; Mitra et al., 2014; Johnson, 2015). Hence, the high abundances of picocyanobacteria,
690 physiologically able to cope with P-limitation, and of potentially mixotrophic dinoflagellates
691 and nanoflagellates, could explain the N and P co-limitation of the communities despite high

DIN:DIP ratios (Burson et al., 2016). Indeed, these physiological and behavioral capacities may have offset an inorganic P-limitation, either by the ingestion of starving preys that may benefit from the added inorganic nutrients, or of dissolved organic substances. This may have led to a N and P co-limitation rather than a single P-limitation (Burson et al., 2016; Fischer et al., 2016). Mixotrophy is also stimulated by nutrient limitation, and would have been particularly competitive in Biguglia lagoon during the three sampling periods. This may explain the bloom of the mixotrophic *Mesodinium rubrum* (Tong et al., 2015; Seong et al., 2017) in the southern basin in the autumn and spring samplings (Fig. 5).

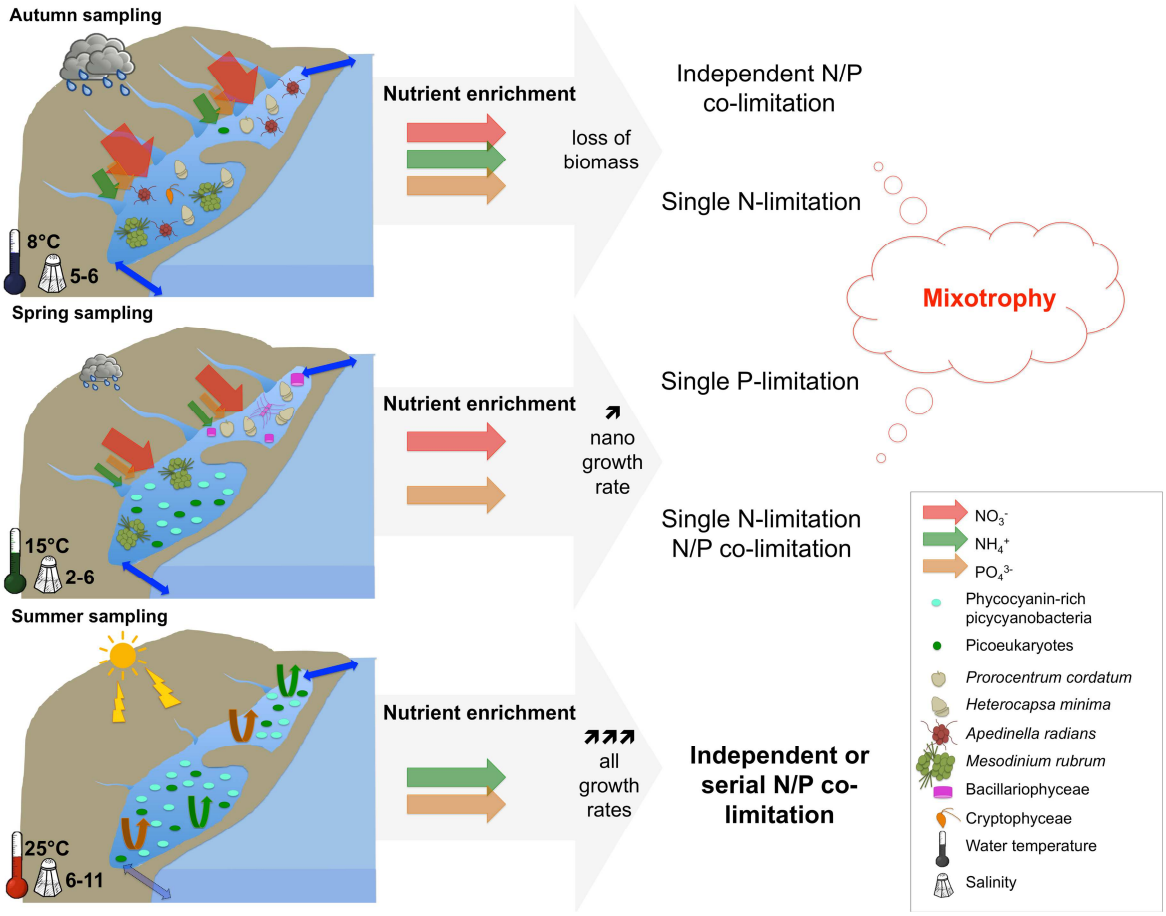

Fig. 5. Schematic representation of the environmental characteristics, phytoplankton community composition and their relationship with nutrient availability during the three bioassays periods in the two stations of Biguglia lagoon. For each sampling, the schematic representation specifies the water temperature, the salinity, the freshwater influence, and the

nutrients inputs whether they come from the watershed or from the sediments. Main phytoplankters are specified as pictograms. Phytoplankton co-limitation by N and P is inferred according to ratios between growth rate under experimentally induced N- or P-limitation and maximal growth rate (see Results).

4.3. *Assumptions about responses of phytoplankton communities to a nutrient pulse*

Bioassay experiments can provide valuable insights about relationship between nutrient dynamics and phytoplankton physiological responses. This can simulate a nutrient pulse, helping to predict algal-based expression of eutrophication (Xu et al., 2012).

The composition of nutrient enrichments used at the three sampling periods was based on previous studies and assumptions about ecosystem functioning, and may have not always reflected the real environmental conditions or the potential nutrient pulses threatening Biguglia lagoon due to its high variability. These enrichments may thus have not always been the most suitable to involve an optimum response of the phytoplankton communities. Hence, the addition of the full enrichment has not always allowed the estimation of maximal growth and mortality rates probably because the underlying assumptions of this method were not always fulfilled. For almost the half of the fractions (11 out of 24) the relationship between the apparent growth rates and the dilution factor was non-linear. Non-linear trends may indicate microzooplankton feeding threshold or saturation depending on the curve pattern (Chen et al., 2014). Indeed, the shape of some of these plots (Fig. S1, red lines) may indicate a strong nutrient limitation and suggests the use of other nutrient resources such as those regenerated through cell lyses, grazing and mineralization that increase with the proportion of undiluted sample (Andersen et al., 1991).

731 The responses of the phytoplankton communities to the nutrient enrichment in the three
732 bioassays have reflected contrasting environmental vulnerability of Biguglia lagoon to short-
733 term nutrient enrichment. Nutrient limitation can have many indirect effects on phytoplankton
734 productivity, *e.g.* a modification of the internal cell stoichiometry that changes its nutritional
735 quality and modify predation rates (Harpole et al., 2011). In November-December 2013, the
736 addition of the full enrichment comprising a mixture of nitrate and ammonium (10 µM each)
737 seems to have had a negative impact. In certain cases, ammonium can negatively affect nitrate
738 uptake and assimilation, especially in nitrate-dominated systems (Domingues et al., 2011;
739 2017), and particularly for dinoflagellates, the least ammonium-tolerant group (Collos and
740 Harrison, 2014). Hence, the addition of ammonium when nitrogen was mainly available as
741 nitrate, and dinoflagellates were the most abundant, may have inhibited its uptake and led to a
742 decrease of growth rate (Dodds and Whiles, 2010; Glibert et al., 2015). As nutrient addition is
743 expected to increase limitation by other resources, a negative response may also reflect
744 strongly constrained N:P stoichiometry. This is suggested by high TN:TP and DIN:DIP
745 values. Rather than re-equilibrating these ratios, nutrient addition may have led to an
746 exacerbated internal stoichiometric imbalance of N and P nutrients with negative impact on
747 phytoplankton growth (Harpole et al., 2011).
748
749 In general, the phytoplankton maximal growth rates followed a predictable seasonal trend,
750 with minima in autumn and maxima in summer. These changes are correlated with water
751 temperatures and photoperiods length, providing more favorable growth conditions in
752 summer. Lower temperatures and light availability in autumn may have altered the uptake rate
753 of phytoplankton (Dodds and Whiles, 2010; Domingues et al., 2011; Reed et al., 2016). This
754 is also consistent with the community composition, the picophytoplankton dominating the
755 community in September potentially having higher growth rate than the nanophytoplankton

dominating the autumn and spring samplings (Bec et al., 2011). Phytoplankton was thus more reactive to a nutrient addition during the summer season when the nutrient demand is the highest. This suggests that Biguglia lagoon is the most vulnerable to nutrient inputs during summer.

Conclusion

Experimental enrichments bioassays are particularly appropriate to explore cause-effect relationships between nutrient availability and phytoplankton dynamics, which can reflect the vulnerability of the whole ecosystem. This is an important issue for managers to draw up appropriate nutrient loading budgets, and to help evaluating the efficiency of subsequent nutrient reduction strategies. In our study, N inputs, particularly NO_3^- during the wet periods and NH_4^+ in summer, stimulated phytoplankton growth in Biguglia lagoon emphasizing the need to mitigate these inputs. The phytoplankton community was strongly influenced by freshwater and nutrients inputs that have led to different physiological and behavioral responses over seasons. During autumn and spring, high DIN:DIP ratios have been associated with blooms of potentially harmful dinoflagellates, which are increasingly observed in Biguglia lagoon.

The absence of a significant positive effect of the enrichment could be explained through several hypotheses. The first is the presence of sufficient amounts of dissolved inorganic nutrients in the water column to sustain the phytoplankton growth during the incubation time. The second could be a more intensive use of other resources than the external pool, such as internal or regenerated inorganic nutrients. The third could be a strong competition for available nutrient with the bacterial communities. Of increasing concern is thus the potential for organic nutrients and high abundances of small preys to promote mixotrophic species,

781 some of which are potentially harmful. It would be important to quantify the availability of
782 dissolved organic nutrients and its effect on phytoplankton growth and trophic modes. This
783 should be linked with a study about the interaction between phytoplankton and bacteria, such
784 as competition for organic and inorganic available nutrients. The impact of bacterial activity
785 on the available nutrients stocks has also to be explored. Indeed, bacterial communities can
786 play an essential role in nutrient cycling, *e.g.* through the remobilization of organic matter,
787 leading to a tight phytoplankton-bacterioplankton coupling (Caroppo, 2002). The possible use
788 of external, internal and regenerated N and P pools, as well as the mixotrophic abilities of the
789 phytoplankton communities also need to be studied.
790

5. Acknowledgements

Amandine Leruste was supported in 2018 by a Postdoctoral fellowship of the University of Corsica Pasquale Paoli (SPE CNRS 6134 Laboratory and UMS Stella Mare) and the Collectivity of Corsica, and from 2013-2016 by a PhD fellowship of the Doctoral School at the University of Montpellier. This work has been financed by Biguglia lagoon nature reserve, the Collectivity of Corsica and the University of Corsica Pasquale Paoli, that authors are grateful for their cooperation. We thank the Ifremer station of Bastia and the UMS Stella Mare for technical support and help during the experiments. This work was (co)funded by the Labex DRIIHM, French programme "Investissements d'Avenir" (ANR-11-LABX-0010) which is managed by the ANR. Thanks are extended to everyone who participated in the experiments. The authors thank the reviewers for their helpful and constructive comments. This research did not receive any specific grant from funding agencies in the public, commercial, or not-for-profit sectors.

All authors have approved the final article.

6. References

Aminot, A., Chaussepied, M.C., 1983. Manuel des analyses chimiques en milieu marin. CNEXO, Brest.

Andersen, K.H., Aksnes, D.L., Berge, T., Fiksen, O., Visser, A., 2015. Modelling emergent trophic strategies in plankton. Journal of Plankton Research 37, 862–868. https://doi.org/10.1093/plankt/fbv054

Andersen, T., Schartau, A., Paasche, E., 1991. Quantifying External and Internal Nitrogen and Phosphorus Pools, as Well. Mar. Ecol.-Prog. Ser. 69, 67–80. https://doi.org/10.3354/meps069067

Anderson, M.J., 2001. A new method for non-parametric multivariate analysis of variance. Austral Ecology 26, 32–46. https://doi.org/10.1111/j.1442-9993.2001.01070.pp.x

Barbier, E.B., Hacker, S.D., Kennedy, C., Koch, E.W., Stier, A.C., Silliman, B.R., 2011. The value of estuarine and coastal ecosystem services. Ecol. Monogr. 81, 169–193. https://doi.org/10.1890/10-1510.1

Bartón, K., 2013. MuMIn: Multi-modal inference. Model selection and model averaging based on information criteria (AICc and alike). http://cran.r-project.org/web/packages/MuMIn/index.html.

Bates, D., Mächler, M., Bolker, B., Walker, S., 2015. Fitting Linear Mixed-Effects Models Using lme4. Journal of Statistical Software 67. https://doi.org/10.18637/jss.v067.i01

826 Bec, B., Collos, Y., Souchu, P., Vaquer, A., Lautier, J., Fiandrino, A., Benau, L., Orsoni, V.,
827 Laugier, T., 2011. Distribution of picophytoplankton and nanophytoplankton along an
828 anthropogenic eutrophication gradient in French Mediterranean coastal lagoons.
829 Aquat. Microb. Ecol. 63, 29–45. https://doi.org/10.3354/ame01480

830 Bec, B., Husseini-Ratrema, J., Collos, Y., Souchu, P., Vaquer, A., 2005. Phytoplankton
831 seasonal dynamics in a Mediterranean coastal lagoon: emphasis on the picoeukaryote
832 community. J. Plankton Res. 27, 881–894. https://doi.org/10.1093/plankt/fbi061

833 Bellinger, E.G., Sigee, D.C. (Eds.), 2015. Freshwater Algae: Identification, Enumeration and
834 Use as Bioindicators. John Wiley & Sons, Inc., Hoboken, NJ, USA.
835 https://doi.org/10.1002/9781118917152

836 Bérard-Therriault, L., Poulin, M., Bossé, L., 1999. Guide d'identification du phytoplancton
837 marin de l'estuaire et du golfe du Saint-Laurent incluant également certains
838 protozoaires Canadian Special Publication of Fisheries and Aquatic Sciences No. 128.
839 NRC Research Press.

840 Burnham, K.P., Anderson, D.R. (Eds.), 2004. Model Selection and Multimodel Inference.
841 Springer New York, New York, NY.

842 Burson, A., Stomp, M., Akil, L., Brussaard, C.P.D., Huisman, J., 2016. Unbalanced reduction
843 of nutrient loads has created an offshore gradient from phosphorus to nitrogen
844 limitation in the North Sea. Limnology and Oceanography 61, 869–888.
845 https://doi.org/10.1002/lno.10257

846 Caroppo, C., 2002. Variability and interactions of phytoplankton and bacterioplankton in
847 Varano lagoon (Adriatic Sea). J Plankton Res 24, 267–273.
848 https://doi.org/10.1093/plankt/24.3.267

849 Cecchi, P., Garrido, M., Collos, Y., Pasqualini, V., 2016. Water flux management and
850 phytoplankton communities in a Mediterranean coastal lagoon. Part II: Mixotrophy of
851 dinoflagellates as an adaptive strategy? Mar. Pollut. Bull.
852 https://doi.org/10.1016/j.marpolbul.2016.04.041

853 Chen, B., Laws, E.A., Liu, H., Huang, B., 2014. Estimating microzooplankton grazing half-
854 saturation constants from dilution experiments with nonlinear feeding kinetics.
855 https://doi.org/10.4319/lo.2014.59.3.0639 59, 639–644.

856 Cloern, J.E., 2001. Our evolving conceptual model of the coastal eutrophication problem.
857 Mar. Ecol.-Prog. Ser. 210, 223–253. https://doi.org/10.3354/meps210223

858 Coelho, S., Gamito, S., Perez-Ruzafa, A., 2007. Trophic state of Foz de Almargem coastal
859 lagoon (Algarve, South Portugal) based on the water quality and the phytoplankton
860 community. Estuar. Coast. Shelf Sci. 71, 218–231.
861 https://doi.org/10.1016/j.ecss.2006.07.017

862 Coelho, S., Perez-Ruzafa, A., Gamito, S., 2015. Phytoplankton community dynamics in an
863 intermittently open hypereutrophic coastal lagoon in Southern Portugal. Estuarine
864 Coastal and Shelf Science 167, 102–112. https://doi.org/10.1016/j.ecss.2015.07.022

865 Collos, Y., Vaquer, A., Bibent, B., Souchu, P., Slawyk, G., Garcia, N., 2003. Response of
866 coastal phytoplankton to ammonium and nitrate pulses: seasonal variations of nitrogen
867 uptake and regeneration. Aquat. Ecol. 37, 227–236.
868 https://doi.org/10.1023/A:1025881323812

869 Collos, Y., Husseini-Ratrema, J., Bec, B., Vaquer, A., Hoai, T.L., Rougier, C., Pons, V.,
870 Souchu, P., 2005. Pheopigment dynamics, zooplankton grazing rates and the autumnal
871 ammonium peak in a Mediterranean lagoon. Hydrobiologia 550, 83–93.
872 https://doi.org/10.1007/s10750-005-4365-1

873 Collos, Y., Bec, B., Jauzein, C., Abadie, E., Laugier, T., Lautier, J., Pastoureaud, A., Souchu,
874 P., Vaquer, A., 2009. Oligotrophication and emergence of picocyanobacteria and a
875 toxic dinoflagellate in Thau lagoon, southern France. J. Sea Res. 61, 68–75.
876 https://doi.org/10.1016/j.seares.2008.05.008

877 Collos, Y., Harrison, P.J., 2014. Acclimation and toxicity of high ammonium concentrations
878 to unicellular algae. Mar. Pollut. Bull. 80, 8–23.
879 https://doi.org/10.1016/j.marpolbul.2014.01.006

880 Collos, Y., Jauzein, C., Ratmaya, W., Souchu, P., Abadie, E., Vaguer, A., 2014. Comparing
881 diatom and Alexandrium catenella/tamarense blooms in Thau lagoon: Importance of
882 dissolved organic nitrogen in seasonally N-limited systems. Harmful Algae 37, 84–91.
883 https://doi.org/10.1016/j.hal.2014.05.008

884 Dodds, W., Whiles, M., 2010. Chapter 16: Nutrient Use and Remineralization, in: Freshwater
885 Ecology - Concepts and Environmental Applications. pp. 437–467.

886 Domingues, R.B., Barbosa, A.B., Sommer, U., Galvao, H.M., 2011. Ammonium, nitrate and
887 phytoplankton interactions in a freshwater tidal estuarine zone: potential effects of
888 cultural eutrophication. Aquat. Sci. 73, 331–343. https://doi.org/10.1007/s00027-011-
889 0180-0

890 Domingues, R.B., Guerra, C.C., Barbosa, A.B., Galvão, H.M., 2017. Will nutrient and light
891 limitation prevent eutrophication in an anthropogenically-impacted coastal lagoon?
892 Continental Shelf Research 141, 11–25.

893 Donald, D.B., Bogard, M.J., Finlay, K., Bunting, L., Leavitt, P.R., 2013. Phytoplankton-
894 Specific Response to Enrichment of Phosphorus-Rich Surface Waters with
895 Ammonium, Nitrate, and Urea. PLoS One 8.
896 https://doi.org/10.1371/journal.pone.0053277

897 Donald, D.B., Bogard, M.J., Finlay, K., Leavitt, P.R., 2011. Comparative effects of urea,
898 ammonium, and nitrate on phytoplankton abundance, community composition, and
899 toxicity in hypereutrophic freshwaters. Limnol. Oceanogr. 56, 2161–2175.
900 https://doi.org/10.4319/lo.2011.56.6.2161

901 Duarte, C.M., Agust, S., Gasol, J.M., Vaqu, D., VazquezDominguez, E., 2000. Effect of
902 nutrient supply on the biomass structure of planktonic communities: an experimental
903 test on a Mediterranean coastal community. Mar Ecol Prog Ser 206, 87–95.
904 https://doi.org/10.3354/meps206087

905 Elser, J.J., Bracken, M.E.S., Cleland, E.E., Gruner, D.S., Harpole, W.S., Hillebrand, H., Ngai,
906 J.T., Seabloom, E.W., Shurin, J.B., Smith, J.E., 2007. Global analysis of nitrogen and
907 phosphorus limitation of primary producers in freshwater, marine and terrestrial
908 ecosystems. Ecology Letters 10, 1135–1142. https://doi.org/10.1111/j.1461-
909 0248.2007.01113.x

910 Erostate, M., Huneau, F., Garel, E., Lehmann, M.F., Kuhn, T., Aquilina, L., Vergnaud-
911 Ayraud, V., Labasque, T., Santoni, S., Robert, S., Provitolo, D., Pasqualini, V., 2018.
912 Delayed nitrate dispersion within a coastal aquifer provides constraints on land-use
913 evolution and nitrate contamination in the past. Science of The Total Environment
914 644, 928–940. https://doi.org/10.1016/j.scitotenv.2018.06.375

915 Fischer, R., Giebel, H., Ptacnik, R., 2016. The identity of the limiting nutrient (N vs. P)
916 affects the competitive success of mixotrophs. Marine Ecology Progress Series.
917 https://doi.org/10.3354/meps11968

918 Franco, A., Fiorin, R., Zucchetta, M., Torricelli, P., Franzoi, P., 2010. Flounder growth and
919 production as indicators of the nursery value of marsh habitats in a Mediterranean
920 lagoon. J. Sea Res. 64, 457–464. https://doi.org/10.1016/j.seares.2010.01.006

921 Garrido, M., Cecchi, P., Collos, Y., Agostini, S., Pasqualini, V., 2016. Water flux
922 management and phytoplankton communities in a Mediterranean coastal lagoon. Part
923 I: How to promote dinoflagellate dominance? Mar. Pollut. Bull. 104, 139–152.
924 https://doi.org/10.1016/j.marpolbul.2016.01.049

925 Glibert, P.M., Wilkerson, F.P., Dugdale, R.C., Raven, J.A., Dupont, C.L., Leavitt, P.R.,
926 Parker, A.E., Burkholder, J.M., Kana, T.M., 2015. Pluses and minuses of ammonium
927 and nitrate uptake and assimilation by phytoplankton and implications for productivity
928 and community composition, with emphasis on nitrogen-enriched conditions. Limnol.
929 Oceanogr. n/a-n/a. https://doi.org/10.1002/lno.10203

930 Guillard, R.R.L., Ryther, J.H., 1962. Studies of Marine Planktonic Diatoms: I. Cyclotella
931 Nana Hustedt, and Detonula Confervacea (cleve) Gran. Can. J. Microbiol. 8, 229–239.
932 https://doi.org/10.1139/m62-029

933 Harpole, W.S., Ngai, J.T., Cleland, E.E., Seabloom, E.W., Borer, E.T., Bracken, M.E.S.,
934 Elser, J.J., Gruner, D.S., Hillebrand, H., Shurin, J.B., Smith, J.E., 2011. Nutrient co-
935 limitation of primary producer communities. Ecology Letters 14, 852–862.
936 https://doi.org/10.1111/j.1461-0248.2011.01651.x

937 Heil, C.A., Glibert, P.M., Fan, C.L., 2005. Prorocentrum minimum (Pavillard) Schiller - A
938 review of a harmful algal bloom species of growing worldwide importance. Harmful
939 Algae 4, 449–470. https://doi.org/10.1016/j.hal.2004.08.003

940 Jeong, H.J., Park, J.Y., Nho, J.H., Park, M.O., Ha, J.H., Seong, K.A., Jeng, C., Seong, C.N.,
941 Lee, K.Y., Yih, W.H., 2005. Feeding by red-tide dinoflagellates on the
942 cyanobacterium Synechococcus. Aquat. Microb. Ecol. 41, 131–143.
943 https://doi.org/10.3354/ame041131

944 Johnson, M.D., 2015. Inducible Mixotrophy in the Dinoflagellate Prorocentrum minimum.
945 Journal of Eukaryotic Microbiology62 62, 431–443.

946 Kemp, W.M., Boynton, W.R., Adolf, J.E., Boesch, D.F., Boicourt, W.C., Brush, G.,
947 Cornwell, J.C., Fisher, T.R., Glibert, P.M., Hagy, J.D., Harding, L.W., Houde, E.D.,
948 Kimmel, D.G., Miller, W.D., Newell, R.I.E., Roman, M.R., Smith, E.M., Stevenson,
949 J.C., 2005. Eutrophication of Chesapeake Bay: historical trends and ecological
950 interactions. Marine ecology. Progress series 303, 1–29.

951 Kjerfve, B., 1994. Coastal Lagoon Processes. Elsevier.

952 Lafabrie, C., Garrido, M., Leboulanger, C., Cecchi, P., Grégori, G., Pasqualini, V., Pringault,
953 O., 2013. Impact of contaminated-sediment resuspension on phytoplankton in the
954 Biguglia lagoon (Corsica, Mediterranean Sea). Estuarine, Coastal and Shelf Science,
955 Pressures, Stresses, Shocks and Trends in Estuarine Ecosystems 130, 70–80.
956 https://doi.org/10.1016/j.ecss.2013.06.025

957 Landry, M., Hassett, R., 1982. Estimating the Grazing Impact of Marine Micro-Zooplankton.
958 Mar. Biol. 67, 283–288. https://doi.org/10.1007/BF00397668

959 Landry, M.R., Brown, S.L., Campbell, L., Constantinou, J., Liu, H., 1998. Spatial patterns in
960 phytoplankton growth and microzooplankton grazing in the Arabian Sea during
961 monsoon forcing. Deep-Sea Research Part Ii-Topical Studies in Oceanography 45,
962 2353–2368. https://doi.org/10.1016/s0967-0645(98)00074-5

963 Le Fur, I., De Wit, R., Plus, M., Oheix, J., Simier, M., Ouisse, V., 2018. Submerged benthic
964 macrophytes in Mediterranean lagoons: distribution patterns in relation to water
965 chemistry and depth. Hydrobiologia 175–200. https://doi.org/10.1007/s10750-017-
966 3421-y

967 Legrand, C., Graneli, E., Carlsson, P., 1998. Induced phagotrophy in the photosynthetic
968 dinoflagellate Heterocapsa triquetra. Aquat. Microb. Ecol. 15, 65–75.
969 https://doi.org/10.3354/ame015065

970 Leruste, A., Malet, N., Munaron, D., Derolez, V., Hatey, E., Collos, Y., De Wit, R., Bec, B.,
971 2016. First steps of ecological restoration in Mediterranean lagoons: Shifts in
972 phytoplankton communities. Estuarine, Coastal and Shelf Science 180, 190–203.
973 https://doi.org/10.1016/j.ecss.2016.06.029

974 Leruste, A., Villéger, S., Malet, N., Wit, R.D., Bec, B., 2018. Complementarity of the
975 multidimensional functional and the taxonomic approaches to study phytoplankton
976 communities in three Mediterranean coastal lagoons of different trophic status.
977 Hydrobiologia 815. https://doi.org/10.1007/s10750-018-3565-4

978 Lin, S., Litaker, R.W., Sunda, W.G., 2015. Phosphorus physiological ecology and molecular
979 mechanisms in marine phytoplankton. Journal of Phycology 52, 10–36.

980 Litchman, E., Klausmeier, C.A., Schofield, O.M., Falkowski, P.G., 2007. The role of
981 functional traits and trade-offs in structuring phytoplankton communities: scaling from
982 cellular to ecosystem level. Ecol. Lett. 10, 1170–1181. https://doi.org/10.1111/j.1461-
983 0248.2007.01117.x

984 Livingston, R.J., 2000. Eutrophication Processes in Coastal Systems: Origin and Succession
985 of Plankton Blooms and Effects on Secondary Production in Gulf Coast Estuaries.
986 CRC Press.

987 Loir, M., 2004. Guide des diatomées: Plus de 200 micro-algues silicieuses photographiées.
988 Delachaux & Niestlé, Paris.

989 Lomas, M.W., Glibert, P.M., 2000. Comparisons of nitrate uptake, storage, and reduction in
990 marine diatoms and flagellates. J. Phycol. 36, 903–913. https://doi.org/10.1046/j.1529-
991 8817.2000.99029.x

992 Maurice, C.F., Bouvier, C., de Wit, R., Bouvier, T., 2013. Linking the lytic and lysogenic
993 bacteriophage cycles to environmental conditions, host physiology and their
994 variability in coastal lagoons. Environ. Microbiol. 15, 2463–2475.
995 https://doi.org/10.1111/1462-2920.12120

996 Mitra, A., Flynn, K.J., Berge, T., Calbet, A., Raven, J.A., Graneli, E., Glibert, P.M., Hansen,
997 P., Stoecker, D.K., Thingstad, T.F., Tillmann, U., Våge, S., Wilken, S., Zubkov, M.V.,
998 2014. The role of mixotrophic protists in the biological carbon pump. Biogeosciences
999 11, 995–1005.

1000 Mouillot, D., Titeux, A., Migon, C., Sandroni, V., Frodello, J.-P., Viale, D., 2000.
1001 Anthropogenic influences on a mediterranean Nature Reserve: modelling and
1002 forecasting. Environmental Modeling & Assessment 5, 185–192.
1003 https://doi.org/10.1023/A:1011533811237

1004 Neveux, J., Lantoine, F., 1993. Spectrofluorometric assay of chlorophylls and phaeopigments
1005 using the least squares approximation technique. Deep Sea Research Part I:
1006 Oceanographic Research Papers 40, 1747–1765. https://doi.org/10.1016/0967-
1007 0637(93)90030-7

1008 Nixon, S.W., 2009. Eutrophication and the macroscope. Hydrobiologia 629, 5–19.
1009 https://doi.org/10.1007/s10750-009-9759-z

1010 Oksanen, J., Blanchet, F., Friendly, M., Kindt, R., Legendre, P., McGlinn, D., Minchin, P.,
1011 O'Hara, R., Simpson, G., Stevens, M., Wagner, H., 2018. vegan: Community Ecology
1012 Package.

1013 Orsoni, V., Souchu, P., Sauzade, D., 2001. Caractérisation de l'état d'eutrophisation des trois
1014 principaux étangs corses (Biguglia, Diana et Urbino), et proposition de renforcement
1015 de leur surveillance. Rapport final.

1016 Paerl, H.W., Dyble, J., Moisander, P.H., Noble, R.T., Piehler, M.F., Pinckney, J.L., Steppe,
1017 T.F., Twomey, L., Valdes, L.M., 2003. Microbial indicators of aquatic ecosystem
1018 change: current applications to eutrophication studies. FEMS Microbiol. Ecol. 46,
1019 233–246. https://doi.org/10.1016/S0168-6496(03)00200-9

1020 Paerl, H.W., Rossignol, K.L., Hall, N.S., Peierls, B.L., Wetz, M.S., 2010. Phytoplankton
1021 Community Indicators of Short- and Long-term Ecological Change in the
1022 Anthropogenically and Climatically Impacted Neuse River Estuary, North Carolina,
1023 USA. Estuaries and Coasts 33, 485–497. https://doi.org/10.1007/s12237-009-9137-0

1024 Pasqualini, V., Derolez, V., Garrido, M., Orsoni, V., Baldi, Y., Etourneau, S., Leoni, V.,
1025 Rébillout, P., Laugier, T., Souchu, P., Malet, N., 2017. Spatiotemporal dynamics of
1026 submerged macrophyte status and watershed exploitation in a Mediterranean coastal

lagoon: Understanding critical factors in ecosystem degradation and restoration. Ecological Engineering 102, 1–14. https://doi.org/10.1016/j.ecoleng.2017.01.027

Patiño, J., Guilhaumon, F., Whittaker, R.J., Triantis, K.A., Gradstein, S.R., Hedenäs, L., González-Mancebo, J.M., Vanderpoorten, A., 2013. Accounting for data heterogeneity in patterns of biodiversity: an application of linear mixed effect models to the oceanic island biogeography of spore-producing plants. Ecography 36, 904–913. https://doi.org/10.1111/j.1600-0587.2012.00020.x

Piehler, M.F., Twomey, L.J., Hall, N.S., Paerl, H.W., 2004. Impacts of inorganic nutrient enrichment on phytoplankton community structure and function in Pamlico Sound, NC, USA. Estuarine, Coastal and Shelf Science 61, 197–209. https://doi.org/10.1016/j.ecss.2004.05.001

R Core Team, 2013. R: A language and environment for statistical computing. R Foundation for Statistical Computing,Vienna, Austria. URL http://www.R-project.org/.

Raven, J.A., 1998. The twelfth Tansley Lecture. Small is beautiful: the picophytoplankton. Funct. Ecol. 12, 503–513. https://doi.org/10.1046/j.1365-2435.1998.00233.x

Reed, M., Pinckney, J.L., Keppler, C., Brock, L., Hogan, S., Greenfield, D., 2016. The influence of nitrogen and phosphorus on phytoplankton growth and assemblage composition in four coastal, southeastern USA systems. Estuarine Coastal and Shelf Science 177, 71–82.

Rochette, S., Rivot, E., Morin, J., Mackinson, S., Riou, P., Le Pape, O., 2010. Effect of nursery habitat degradation on flatfish population: Application to Solea solea in the Eastern Channel (Western Europe). Journal of Sea Research 64, 34–44. https://doi.org/10.1016/j.seares.2009.08.003

Schramm, W., 1999. Factors influencing seaweed responses to eutrophication: some results from EU-project EUMAC. Journal of Applied Phycology 11, 69–78. https://doi.org/10.1023/A:1008076026792

Seong, K.A., Myung, G., Jeong, H.J., Yih, W., Kim, H.S., Park, J.Y., Yoo, Y.D., 2017. Ingestion rate and grazing impact by the mixotrophic ciliate Mesodinium rubrum on natural populations of marine heterotrophic bacteria in the coastal waters of Korea. Algae 32, 47–55.

Sorokin, Y., Dallocchio, F., 2008. Dynamics of phosphorus in the Venice lagoon during a picocyanobacteria bloom. Journal of Plankton Research 30, 1019–1026.

Souchu, P., Bec, B., Smith, V.H., Laugier, T., Fiandrino, A., Benau, L., Orsoni, V., Collos, Y., Vaquer, A., 2010. Patterns in nutrient limitation and chlorophyll a along an anthropogenic eutrophication gradient in French Mediterranean coastal lagoons. Can. J. Fish. Aquat. Sci. 67, 743–753. https://doi.org/10.1139/F10-018

Tomas, C.R., 1997. Identifying Marine Phytoplankton. Academic Press.

Tong, M., Smith, J., Anderson, D.M., 2015. Role of dissolved nitrate and phosphate in isolates of Mesodinium rubrum and toxin-producing Dinophysis acuminata. Aquatic Microbial Ecology 75, 169–185.

1067 Xu, J., Yin, K., Lee, J.H.W., Anderson, D.M., Jiang, Y., Yuan, X., Ho, A.Y.T., Harrison, P.J.,
1068 2012. Resistance of Hong Kong waters to nutrient enrichment: assessment of the role
1069 of physical processes in reducing eutrophication. J. Oceanogr. 68, 545–560.
1070 https://doi.org/10.1007/s10872-012-0118-8.

1071

7. Supplementary material

Table S1. Net growth rates (μ_0) measured in incubations without enrichment and maximal growth (μ_{max}) and mortality rates (g) subsequently calculated using full N and P enrichment in the two NB and SB stations of Biguglia lagoon. Values were estimated according the linear Landry and Hasset (1982) equation. This model has been compared to alternative models by mixed-effect multiple linear regressions of apparent growth rates, based on Chl *a* concentration from dilution experiments. The parsimony of the different models was checked by the AIC criterion. The linear model was only accepted when it presented a delta-AIC_c, <2 with respect to the most parsimonious model (see Methods). AIC_c–w describe the strength of explanation by the model of the model. R^2: coefficient of determination. The μ_0:μ_{max} ratio reflects the impact of the nutrient enrichment on the phytoplankton growth (1: no effect; 0: high enhancement of growth), highlighting the nutrient limitation under natural conditions. ****p*-value <0.001, ***p*-value <0.01, **p*-value <0.05.

Stations	Samplings	Fraction	μ_0	μ_{max}	g	n	AICc	ΔAICc	AICc-w	R^2	μ_0 :μ_{max}
			(d^{-1})								
NB	Nov - Dec 2013	**Tot**	**0.45**	**<0**	**0.62**	**8**	**11.5**	**1.45**	**0.33**	**0.31 .**	**<0**
		Micro	<0	<0	1.45	7	37.1	6.05	0.04	-0.05	-
		Nano	0.37	0.46	0.26	8	6.4	3.54	0.13	0.10	0.79
		Ultra	**0.96**	**<0**	**1.82**	**8**	**24.7**	**0.00**	**0.55**	**0.45***	**<0**
	April 2014	Tot	<0	0.25	<0	7	1.4	4.25	0.10	0.19	<0
		Micro	<0	0.24	1.01	8	24.0	2.39	0.19	0.13	<0
		Nano	**1.13**	**1.83**	**0.28**	**8**	**-5.2**	**0.00**	**0.50**	**0.53***	**0.62**
		Ultra	<0	<0	0.43	8	9.9	2.26	0.21	0.23	-
	September 2014	**Tot**	**0.64**	**1.78**	**0.30**	**9**	**-10.7**	**0.00**	**0.68**	**0.64****	**0.36**
		Micro	**1.84**	**3.40**	**0.57**	**9**	**3.2**	**0.00**	**1.00**	**0.58***	**0.54**
		Nano	**1.60**	**2.70**	**0.57**	**9**	**-4.1**	**0.00**	**1.00**	**0.76****	**0.59**
		Ultra	**0.51**	**1.12**	**0.45**	**8**	**2.20**	**0.86**	**0.39**	**0.48***	**0.45**
SB	Nov - Dec 2013	**Tot**	**0.48**	**0.41**	**0.69**	**10**	**1.7**	**0.00**	**0.54**	**0.65****	**1.19**
		Micro	1.12	0.45	1.12	9	45.3	4.40	0.09	-0.09	2.48
		Nano	1.17	0.90	0.50	10	20.3	2.62	0.18	0.05	1.30
		Ultra	**<0**	**0.14**	**1.10**	**8**	**9.3**	**0.00**	**0.93**	**0.70****	**<0**
	April 2014	Tot	0.17	0.19	<0	7	15.1	5.18	0.07	0.08	0.92
		Micro	-	-	-	-	-	-	-	-	-
		Nano	**1.91**	**2.00**	**0.83**	**7**	**12.8**	**0.37**	**0.33**	**0.59***	**0.95**
		Ultra	<0	0.01	<0	8	14.3	4.46	0.09	-0.01	<0
	September 2014	**Tot**	**<0**	**1.79**	**0.16**	**7**	**-21.1**	**0.45**	**0.44**	**0.88****	**<0**
		Micro	0.39	10.08	0.39	9	27.9	4.80	0.05	-0.09	0.04
		Nano	**1.42**	**3.23**	**1.14**	**10**	**11.6**	**0.69**	**0.40**	**0.65****	**0.44**
		Ultra	**<0**	**0.87**	**<0**	**10**	**9.6**	**0.67**	**0.32**	**0.38***	**<0**

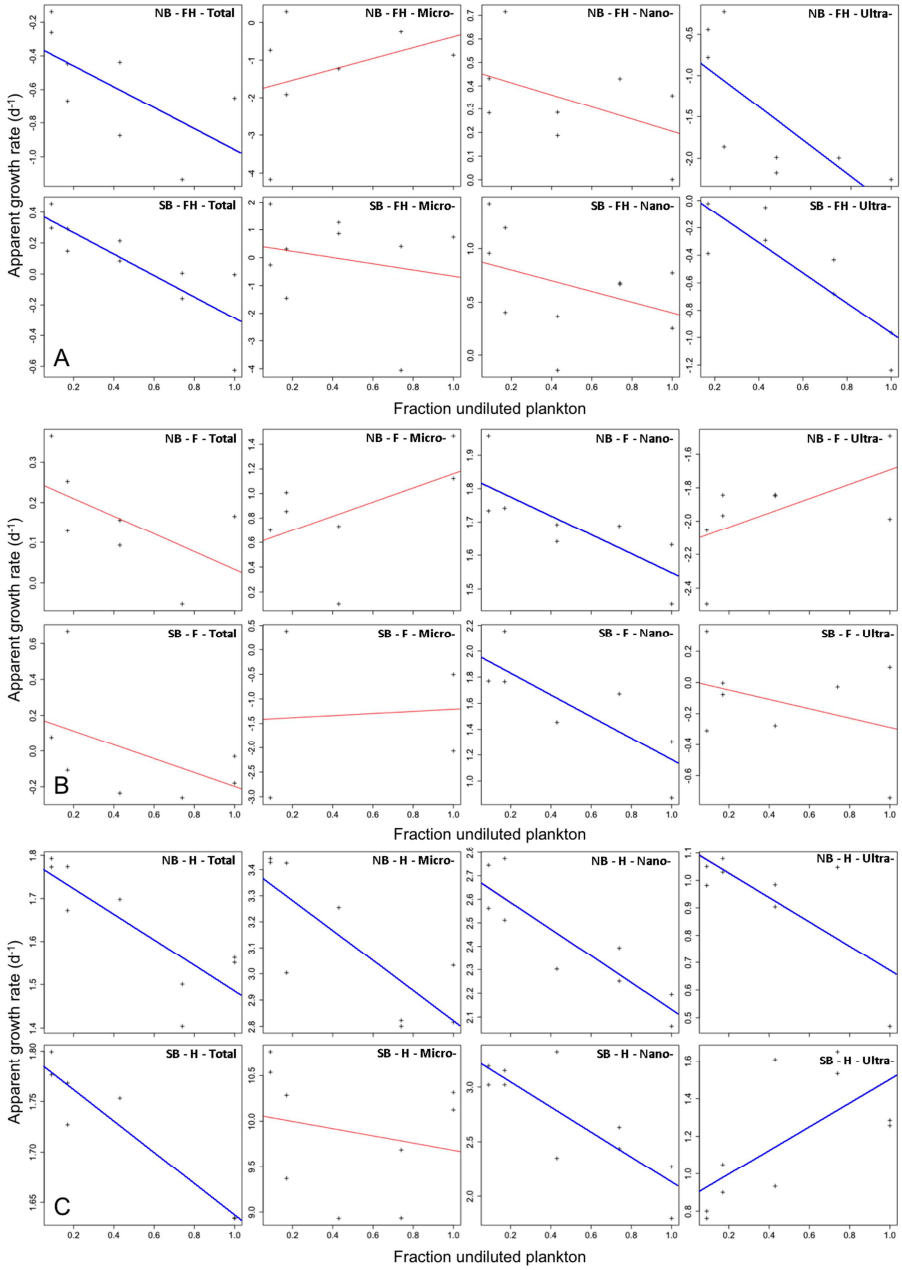

Fig. S1. Apparent growth rate as a function of the dilution factor in bioassays with full N and P enrichment in NB and SB station of Biguglia lagoon in (A) November-December 2013, (B) April 2014, and (C) September 2014. From the left to the right, total phytoplankton, microphytoplankton >20 µm, nanophytoplankton between 5 and 20 µm, and ultraphytoplankton <5 µm. The line corresponds to the linear equation $k(x) = \mu_{max} - gx$, with k the apparent growth rate, x the fraction of undiluted plankton, μ_{max} (as Y axis intercept) the maximum growth rate, and g the grazing rate. Blue lines highlight when the linear model best-fitted the relationship between the apparent growth rates and the dilution factors.

1094 Table S2. Net growth (μ_{-N}) and mortality rates (g) subsequently calculated using enrichment
1095 minus N in the two NB and SB stations of Biguglia lagoon. Values were estimated according
1096 the equations from Andersen et al. (1991). The linear model has been compared to alternative
1097 models by mixed-effect multiple linear regressions of apparent growth rates, based on Chl *a*
1098 concentration from dilution experiments. The parsimony of the different models was checked
1099 by the AIC criterion. The linear model was only accepted when it presented a delta-AIC_c, <2
1100 with respect to the most parsimonious model (see Methods). AIC_c–w describe the strength of
1101 explanation by the model of the model. R^2: coefficient of determination. ****p*-value <0.001,
1102 ***p*-value <0.01, **p*-value <0.05.

Stations	Samplings	Fraction	μ_{-N}	g	n	AIC_c	ΔAIC_c	AIC_c-w	R_2
			(d^{-1})						
NB	Nov - Dec 2013	Total	<0	0.19	8	-5.3	1.75	0.30	0.28
		Micro-	<0	1.70	6	-	-	-	-0.13
		Nano-	0.62	0.29	8	-9	0,00	0.93	0.70**
		Ultra-	<0	1.82	8	24.7	0,00	0.55	0.45*
	April 2014	Total	0.51	0.71	9	-5	0,00	1,00	0.84***
		Micro-	1.59	2.57	8	19.4	0,00	0.93	0.70**
		Nano-	1.95	0.83	10	-6.1	0,00	1,00	0.86***
		Ultra-	-1.59	0.13	8	-	-	-	-0.03
	September 2014	Total	0.86	0.71	10	-1.3	0,00	0.99	0.73**
		Micro-	1.78	0.55	9	10	0.02	0.50	0.33 .
		Nano-	1.77	0.99	10	12.6	0,00	0.93	0.56**
		Ultra-	0.51	0.73	9	1.3	0,00	0.98	0.73**
SB	Nov - Dec 2013	Total	0.26	0.39	10	-9.7	0,00	0.98	0.65**
		Micro-	1.09	2.14	9	35.8	0.38	0.45	0.30 .
		Nano-	0.78	0.15	9	-	-	-	-0.08
		Ultra-	1.85	0.82	10	3.1	0,00	0.99	0.69**
	April 2014	Total	0.06	0.03	9	-	-	-	-0.14
		Micro-	-	-	-	-	-	-	-
		Nano-	1.64	0.42	10	-	-	-	0.08
		Ultra-	0.10	0.50	9	4.1	0,00	0.71	0.45*
	September 2014	Total	0.28	1.06	10	1.2	0,00	1.00	0.83***
		Micro-	9.80	1.11	10	8.7	0,00	0.99	0.70**
		Nano-	1.58	1.01	10	-3.6	0,00	1,00	0.87***
		Ultra-	<0	1.25	10	7.1	0,00	1.00	0.78***

1103 Table S3. Net growth (μ_{-P}) and mortality rates (g) subsequently calculated using enrichment
1104 minus P in the two NB and SB stations of Biguglia lagoon. Values were estimated according
1105 the equations from Andersen et al. (1991). The linear model has been compared to alternative
1106 models by mixed-effect multiple linear regressions of apparent growth rates, based on Chl *a*
1107 concentration from dilution experiments. The parsimony of the different models was checked
1108 by the AIC criterion. The linear model was only accepted when it presented a delta-AIC_c, <2
1109 with respect to the most parsimonious model (see Methods). AIC_c–w describe the strength of
1110 explanation by the model of the model. R^2: coefficient of determination. ****p*-value <0.001,
1111 ***p*-value <0.01, **p*-value <0.05.

Stations	Samplings	Fraction	μ_{-P}	g	n	AIC_c	ΔAIC_c	AIC_c-w	R^2
			(d^{-1})						
NB	Nov - Dec 2013	Total	0.30	0.24	9	-1.9	1.16	0.36	0.24
		Micro-	<0	<0	10	-	-	-	-0.12
		Nano-	1.13	0.44	10	1.9	0,00	0.74	0.40*
		Ultra-	<0	<0	10	-	-	-	-0.12
	April 2014	Total	0.07	0.41	8	1.9	0,00	0.65	0.50*
		Micro-	1.01	1.46	4	-	-	-	0.27
		Nano-	1.54	0.44	8	8.2	1.35	0.34	0.31
		Ultra-	<0	0.53	6	7.4	1.14	0.36	0.71*
	September 2014	Total	1.03	0.24	10	-4.8	0.15	0.48	0.26 .
		Micro-	2.24	0.58	10	12.3	0.01	0.50	0.27
		Nano-	2.13	0.29	10	-5.2	0,00	0.67	0.37*
		Ultra-	0.52	0.31	9	-0.1	0.12	0.49	0.32 .
SB	Nov - Dec 2013	Total	0.53	0.78	10	-0.6	0,00	1.00	0.75***
		Micro-	1.05	2.65	9	25.7	0,00	0.95	0.65**
		Nano-	1.07	0.48	10	3.5	0,00	0.74	0.40*
		Ultra-	2.02	0.83	10	5.2	0,00	0.98	0.65**
	April 2014	Total	0.26	0.57	9	-9.5	0,00	1.00	0.86***
		Micro-	-	-	-	-	-	-	-
		Nano-	1.64	0.52	9	3	0,00	0.83	0.53*
		Ultra-	0.34	0.69	9	-7	0,00	1.00	0.87***
	September 2014	Total	1.34	0.03	9	-	-	-	-0.14
		Micro-	11.72	-0.17	10	-	-	-	-0.06
		Nano-	<0	2.45	8	-	-	-	0.15
		Ultra-	<0	0.19	9	-4.6	1.65	0.30	0.19

1112

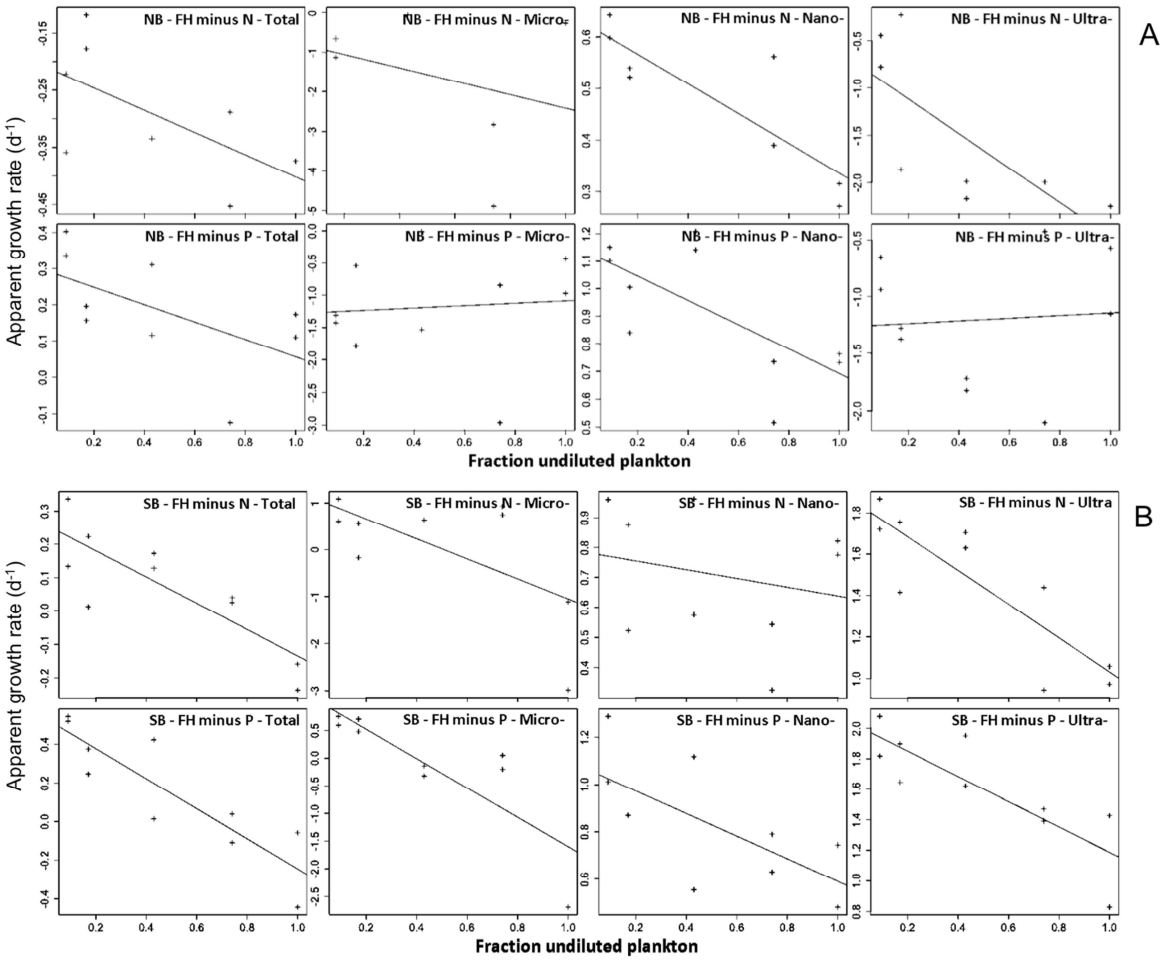

Fig. S2. Apparent growth rate as a function of the dilution factor in bioassays with full FH enrichment minus N and minus P, in the NB (A) and SB (B) stations of Biguglia lagoon in November-December 2013. From the left to the right, total phytoplankton, microphytoplankton >20 µm, nanophytoplankton between 5 and 20 µm, and ultraphytoplankton <5 µm. The line corresponds to the linear equation $k(x) = \mu - gx$, with k the apparent gross growth rate, x the fraction of undiluted plankton, μ (as Y axis intercept) the gross growth rate, and g the grazing rate. However, we assume that this model can not best-fit the relationship between apparent growth rate and fraction of undiluted plankton in nutrient limiting conditions, due to the potential use of alternative resources (Andersen et al., 1991).

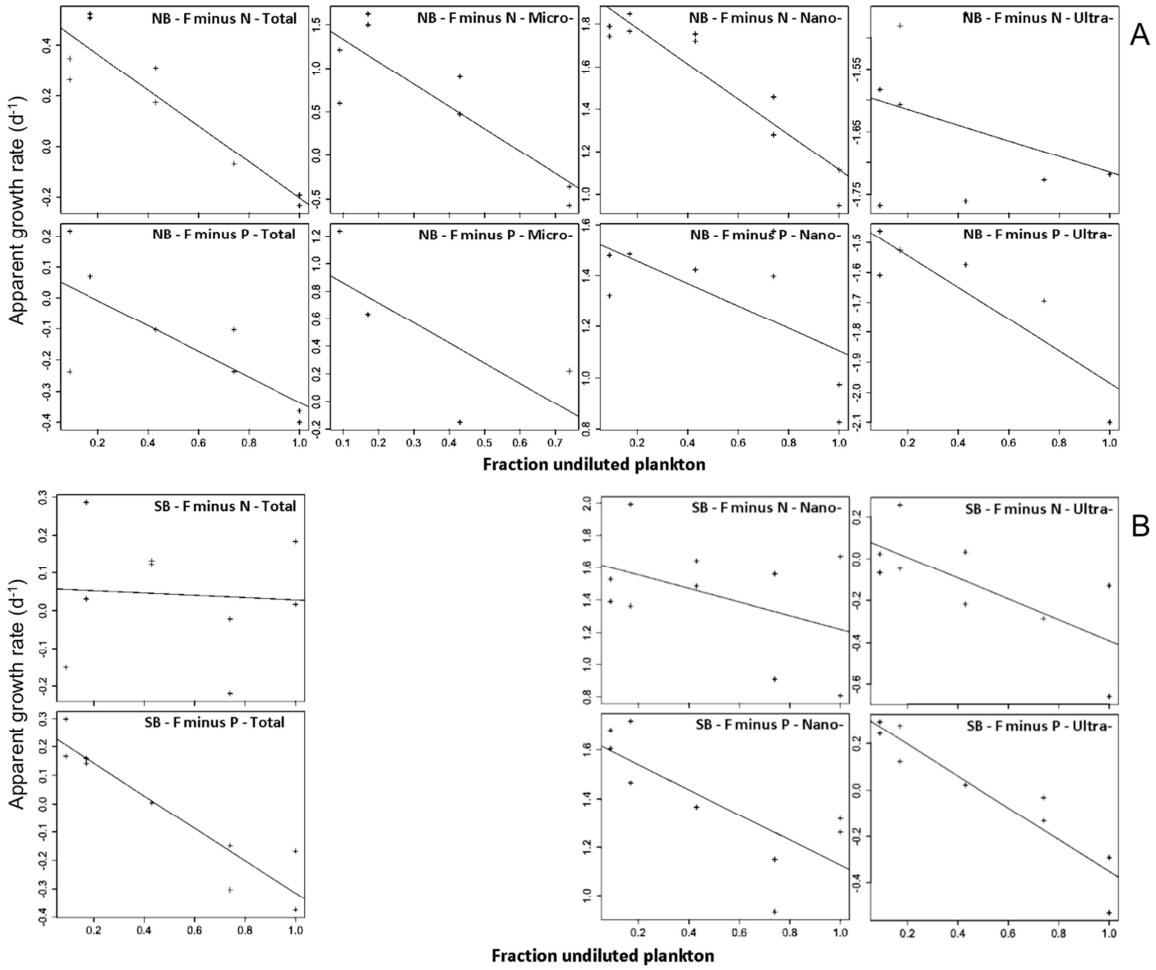

Fig. S3. Apparent growth rate as a function of the dilution factor in bioassays with full F enrichment minus N and minus P, in the NB (A) and SB (B) stations of Biguglia lagoon in April 2014. From the left to the right, total phytoplankton, microphytoplankton >20 µm (absent in SB), nanophytoplankton between 5 and 20 µm, and ultraphytoplankton <5 µm. The line corresponds to the linear equation $k(x) = \mu - gx$, with k the apparent gross growth rate, x the fraction of undiluted plankton, μ (as Y axis intercept) the gross growth rate, and g the grazing rate. However, we assume that this model can not best-fit the relationship between apparent growth rate and fraction of undiluted plankton in nutrient limiting conditions, due to the potential use of alternative resources (Andersen et al., 1991).

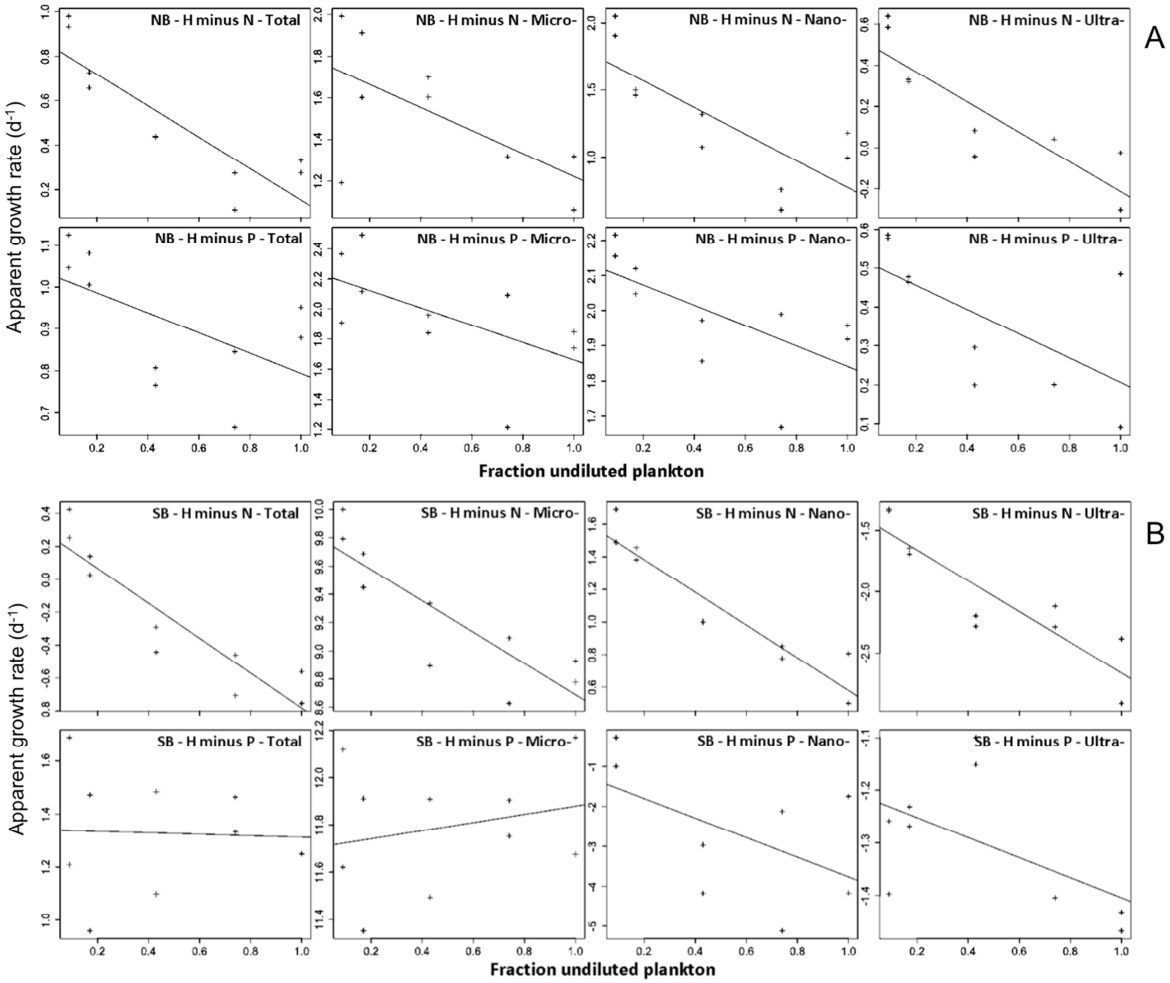

Fig. S4. Apparent growth rate as a function of the dilution factor in bioassays with full H enrichment minus N and minus P, in the NB (A) and SB (B) stations of Biguglia lagoon in September 2014. From the left to the right, total phytoplankton, microphytoplankton >20 µm, nanophytoplankton between 5 and 20 µm, and ultraphytoplankton <5 µm. The line corresponds to the linear equation $k(x) = \mu - gx$, with k the apparent growth rate, x the fraction of undiluted plankton, μ (as Y axis intercept) the growth rate, and g the grazing rate. However, we assume that this model can not best-fit the relationship between apparent growth rate and fraction of undiluted plankton in nutrient limiting conditions, due to the potential use of alternative resources (Andersen et al., 1991).